The Journal of Experimental Biology 207, 4343-4360
Published by The Company of Biologists 2004
doi:10.1242/jeb.01292

Rapid evolution of muscle fibre number in post-glacial populations of Arctic charr *Salvelinus alpinus*

Ian A. Johnston[1,*], Marguerite Abercromby[1], Vera L. A. Vieira[1], Rakel J. Sigursteindóttir[2], Bjarni K. Kristjánsson[2], Dean Sibthorpe[1] and Skúli Skúlason[2]

[1]*Gatty Marine Laboratory, School of Biology, University of St Andrews, St Andrews, Fife, KY16 8LB, Scotland, UK* and [2]*Holar University College, 551 Skagafjordur, Iceland*

*Author for correspondence (e-mail: iaj@st-andrews.ac.uk)

Accepted 17 September 2004

Summary

Thingvallavatn, the largest and one of the oldest lakes in Iceland, contains four morphs of Arctic charr *Salvelinus alpinus*. Dwarf benthic (DB), large benthic (LB), planktivorous (PL) and piscivorous (PI) morphs can be distinguished and differ markedly in head morphology, colouration and maximum fork length (FL_{max}), reflecting their different resource specialisations within the lake. The four morphs in Thingvallavatn are thought to have been isolated for approximately 10 000 years, since shortly after the end of the last Ice Age.

We tested the null hypothesis that the pattern of muscle fibre recruitment was the same in all morphs, reflecting their recent diversification. The cross-sectional areas of fast and slow muscle fibres were measured at 0.7 *FL* in 46 DB morphs, 23 LB morphs, 24 PL morphs and 22 PI morphs, and the ages of the charr were estimated using sacculus otoliths. In fish larger than 10 g, the maximum fibre diameter scaled with body mass $(M_b)^{0.18}$ for both fibre types in all morphs. The number of myonuclei per cm fibre length increased with fibre diameter, but was similar between morphs. On average, at 60 μm diameter, there were 2264 nuclei cm^{-1} in slow fibres and 1126 nuclei cm^{-1} in fast fibres. The absence of fibres of diameter 4–10 μm was used to determine the *FL* at which muscle fibre recruitment stopped. Slow fibre number increased with body length in all morphs, scaling with $M_b^{0.45}$. In contrast, the recruitment of fast muscle fibres continued until a clearly identifiable *FL*, corresponding to 18–19 cm in the dwarf morph, 24–26 cm in the pelagic morph, 32–33 cm in the large benthic morph and 34–35 cm in the piscivorous morph. The maximum fast fibre number (FN_{max}) in the dwarf morph (6.97×10^4) was 56.5% of that found in the LB and PI morphs combined (1.23×10^5) ($P<0.001$). Muscle fibre recruitment continued until a threshold body size and occurred at a range of ages, starting at 4+ years in the DB morph and 7+ years in the LB and PI morphs. Our null hypothesis was therefore rejected for fast muscle and it was concluded that the dwarf condition was associated with a reduction in fibre number.

We then investigated whether variations in development temperature associated with different spawning sites and periods were responsible for the observed differences in muscle cellularity between morphs. Embryos from the DB, LB and PL morphs were incubated at temperature regimes simulating cold subterranean spring-fed sites (2.2–3.2°C) and the general lakebed (4–7°C). Myogenic progenitor cells (MPCs) were identified using specific antibodies to Paired box protein 7 (Pax 7), Forkhead box protein K1-α (FoxK1-α), MyoD and Myf-5. The progeny showed no evidence of developmental plasticity in the numbers of either MPCs or muscle fibres. Juveniles and adult stages of the DB and LB morphs coexist and have a similar diet. We therefore conclude that the reduction in FN_{max} in the dwarf morph probably has a genetic basis and that gene networks regulating myotube production are under high selection pressure. To explain these findings we propose that there is an optimal fibre size, and hence number, which varies with maximum body size and reflects a trade-off between diffusional constraints on fibre diameter and the energy costs of maintaining ionic gradients. The predictions of the optimal fibre size hypothesis and its consequences for the adaptive evolution of muscle architecture in fishes are briefly discussed.

Key words: muscle fibres, myogenesis, growth, myogenic progenitor cell, resource polymorphism, developmental plasticity, fish, Arctic charr, myogenic regulatory factor, Paired box protein 7, Forkhead box protein K1-α.

Introduction

The Arctic charr *Salvelinus alpinus* L. is the most northerly distributed freshwater fish with a holoArctic distribution. The species shows marked phenotypic diversity in morphology, life history and behaviour between populations (Johnson, 1980;

Skúlason et al., 1999). Glaciers covered most of the current geographical range of the species until the end of the Pleistocene, around 10 000 years ago. Mitochondrial DNA sequence variation points to a common Atlantic lineage that diverged from other charr lineages in the early to mid-Pleistocene, and subsequently underwent rapid diversification as new freshwater habitats became available at the end of the last Ice Age (Brunner et al., 2001). Consistent with this hypothesis, the genotyping of populations at six microsatellite loci has revealed low levels of genetic structuring of populations between regions, but high levels between and within lakes (Wilson et al., 2004). Wilson et al. (2004) found that in lakes containing discrete morphs there was evidence for sympatric populations in ten lakes, and multilocus heterozygote deficits in a further 23 lakes in Iceland, Scandinavia and Scotland, which suggests that separate breeding populations might be relatively common.

Thingvallavatn (64°11′N, 21°08′W) is situated along an exposed part of the Mid-Atlantic Ridge system and is Iceland's largest lake (83 km^2). Since its formation approximately 10 000 years ago tectonic drift and associated volcanic activity has determined its size and topology, and it is thought to have become isolated from other freshwater systems approximately 9000 years ago (Saemundsson, 1992). The present day lake is dominated by Arctic charr, which are found in most available habitats. Threespine sticklebacks *Gasterosteus aculeatus* L. are also common in the lake, both in sheltered locations and in the *Nitella opaca* zone on the bottom. There is also a small population of brown trout *Salmo trutta* L. in the lake (Sandlund et al., 1992). The four morphs of Arctic charr found in Thingvallavatn (Fig. 1) represent an extreme case of phenotypic diversification that is thought to have evolved because of relaxed interspecific competition for available resources, but increased intraspecific competiton (Skúlason and Smith, 1995). Two morphs, a dwarf benthic (DB) and a large benthic (LB) form, have trophic specialisations for bottom feeding, and can be identified by having blunt snouts, a sub-terminal mouth and large pectoral fins (Fig. 1). The DB morph can effectively exploit the interstitial habitat of lava fissures at the bottom of the lake for food and shelter whereas LB charr with its larger body size must forage above the stone matrix (Sandlund et al., 1992). There are also two 'pelagic morphotypes' (Fig. 1), the planktivorous (PL) and piscivorous (PI) morphs, which have terminal mouths (longer lower jaws) and smaller pectoral fins than the benthic morphs (Sandlund et al., 1992; Snorrason et al., 1994). The pelagic morphs fit within the range of morphological variation shown for Arctic charr in general, and are probably closest to the ancestral condition (Snorrason and Skúlason, 2004). The four morphs also differ in colouration, growth rate, foraging behaviour, age at first sexual maturity and maximum body length (Sandlund et al., 1992). Female DB morphs start to spawn at 7.5 cm, at 2–4 years of age, and can reach 27 cm fork length (*FL*), whereas the female LB morphs start to spawn at 30 cm, at age 6–10 years, and can reach 54 cm *FL* (Sandlund et al., 1992; Snorrason and Skúlason, 2004). Differences in spawning time, spawning location and assortative mating behaviours may result in reproductive isolation of the morphs (Skúlason et al., 1989a), a hypothesis that is at least partially supported by genetic data (Wilson et al., 2004). Local origin of morphs is supported by several studies on other lakes containing polymorphic charr (Gíslason et al., 1999; Wilson et al., 2004). Common garden rearing experiments indicate that the differences in morphology, growth and behaviour between the morphs have a strong genetic component (Skúlason et al., 1989b, 1993, 1996; Eiríksson et al., 1999).

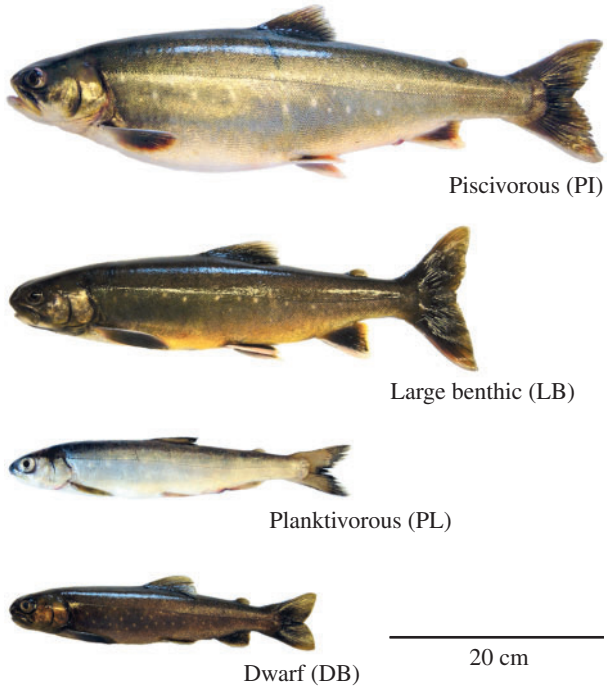

Fig. 1. The four morphs of Arctic charr *Salvelinus alpinus* L. found in Lake Thingvallavatn, Iceland. The specimens of piscivorous (PI), large benthic (LB), planktivorous (PL) and dwarf benthic (DB) morph illustrated are close to the maximum body size found. The distinct head and fin morphology and the different colouration of the different morphs used in their classification is readily apparent.

Fish myotomes contain two or more muscle fibre types arranged in discrete layers, each with different metabolic and contractile profiles and roles in swimming (Johnston et al., 1977). Myotubes are formed in three discrete phases during ontogeny (Rowlerson and Veggetti, 2001; Johnston and Hall, 2004). Following a purely embryonic phase of myogenesis (Devoto et al., 1996; Blagden et al., 1997; Johnston et al., 1997), additional fibres are produced from discrete germinal zones by stratified hyperplasia until the larval or early juvenile stages (Rowlerson et al., 1995; Johnston and McLay, 1997; Johnston et al., 1998; Barresi et al., 2001; Johnston and Hall, 2004). The final and most prolonged phase of myotube formation, termed mosaic hyperplasia, can continue past sexual maturity and involves a general activation of myogenic progenitor cells (MPCs) throughout the myotome (Rowlerson et al., 1995; Johnston et al., 1998, 2003d).

Body size is expected to have a major impact on the maximum number and size of the myotomal muscle fibres (Weatherley et al., 1980, 1988; Johnston et al., 2003a). In ten species of North American freshwater fish representing diverse taxa, muscle fibre recruitment was found to continue until 44% of the maximum fork length (Weatherley et al., 1988). Similarly, in species showing marked sexual dimorphism in body size, such as the Argentine hake *Merluccius hubbsi*, muscle fibre recruitment continued for longer in females, which are larger (Calvo, 1989). In a study of 16 species of notothenioid fish (Perciformes) with sub-Antarctic and Antarctic distributions, body length was found to explain 69% of the total variation in the maximum number of fast muscle fibres (FN_{max}) (Johnston et al., 2003a). Antarctic notothenioids contain 'giant muscle fibres' reflecting the relaxation of diffusional constraints at low temperature (Smialovska and Kilarski, 1981; Egginton et al., 2002; Johnston, 2003). Phylogenetically based statistical methods revealed a corresponding and dramatic reduction in size-corrected FN_{max} in the lineage leading to the Channichthyidae (Johnston et al., 2003a). FN_{max} in the icefish *Chaenocephalus aceratus* was only 7.7% of that in *Eleginops maclovinus,* a basal sub-Antarctic notothenioid that reaches the same maximum length (Johnston et al., 2003a). Molecular phylogenies provide strong evidence that species from the core radiation of Antarctic notothenioids have invaded warmer sub-Antarctic waters over the last few million years (Bargelloni et al., 1994, 2000; Stankovic et al., 2001). However, these species have apparently retained the low fibre number and large maximum fibre size characteristic of the Antarctic species (Johnston et al., 2003a).

Since the four morphs of Arctic charr in Thingvallavatn originated in the lake during the last 10 000 years they provide an excellent model to study evolutionary processes leading to population formation and possibly speciation (Skúlason et al., 1999). Given the great variation in size and growth patterns among morphs it is interesting to examine possible differences in the evolution of muscle architecture. In the present study, we tested the null hypothesis that muscle cellularity was the same in all morphs of Arctic charr in Thingvallavatn, reflecting their recent diversification. The number of muscle fibres formed at each phase of myogenesis is sensitive to egg incubation temperature (Stickland et al., 1988; Johnston et al., 2000a,b, 2003c; Johnston and Hall, 2004). Variation in spawning time and the influence of cold groundwater on spawning sites give rise to the possibility of differences in development temperature between morphs (Skúlason et al., 1989a). We therefore also investigated the possibility of temperature-induced plasticity in muscle development between the morphs.

Materials and methods

Fish

Arctic charr *Salvelinus alpinus* L. were caught using electrofishing (juveniles) and gill nets (mesh sizes 10 mm, 12.5 mm, 15.5 mm, 19.5 mm, 24 mm, 29 mm, 35 mm, 43 mm and 55 mm) in various locations around Thingvallavatn, Iceland. Fishing took place in 2001 (June), 2002 (June and August) and 2003 (June/July). Fish were either killed at the lakeside or transported live to Holar University College in tanks of oxygenated water and then sampled within 3 days of capture. Fish were killed by stunning and pithing of the central nervous system. Morphs were identified on the basis of head and fin morphology, colouration and stomach contents (Sandlund et al., 1992). The DB and LB morphs were feeding on the snail *Lymnaca peregra* and other benthic invertebrates. The stomachs of the PL and PI morphs contained pelagic crustaceans and sticklebacks, respectively.

Age determination

The age of the charr were estimated from sacculus otoliths. The otoliths were read whole in glycerol under a blue light as described by Jonsson (1976).

Rearing experiments

Eggs from ovulating females of DB, LB and PL morphs were stripped at the Holar University Aquarium. Eggs from 21 LB, 20 DB and 23 PL morphs were fertilised *in vitro* using sperm from a unique male of the same morph. After 1 h of hydration in water, eggs were split into two and each half transferred to two development chambers containing incubation troughs partitioned with 1 mm mesh. Fertilised eggs were separated into families between partitions. The chambers were fed by a continuous flow of water from an underground spring and maintained at either 2.2–3.2°C, simulating the groundwater-fed spawning sites in Thingvallavatn, or in heated water at 4–7°C (range, decreasing during development), simulating the general lake temperature. The progeny of all morphs experienced identical temperatures. Eggs were incubated in the dark, and regularly bathed with Malachite–Green Oxalate (Merk, kGaA; VWR International, Lutterworth, Leicester, UK) to prevent fungal infection. After hatching, fry were transferred to 1 m-diameter flow-through tanks, and families were separated into 0.5 l open containers with a 1 mm-mesh bottom at ambient temperature (4–6°C) and ambient photoperiod.

Histology

A 0.5 cm transverse steak of the trunk was prepared at 0.7 fork length (*FL*) using a sharp knife. The steak was photographed on a light box using a digital camera and the total cross-sectional area (TCA) of each fibre type muscle was digitised. Up to 8 blocks (5×5 mm^2) were made from the steak so as to representatively sample all areas of the myotome. The number of blocks was adjusted to sample 50–100% of one half of the fast muscle. The blocks included 80–100% of the total cross-sectional of slow muscle. Blocks were frozen in isopentane (2-methyl butane) cooled to near its freezing point in liquid nitrogen (–159°C). Frozen sections were cut on a cryostat at 8 μm thickness.

Enzyme histochemistry

Sections were stained for succinic dehydrogenase activity (Nachlas et al., 1957) and for glycogen, using the Periodic Acid

Schiff's method (Pearse, 1960). Sections were stained for myosin ATPase (mATPase) with and without preincubation at pH 4.3 (30 s to 2 min) or pH 10.2 (30 s to 2 min) (Johnston et al., 1974).

Electron microscopy

Small bundles of slow and fast muscle fibres were pinned at their resting length *in situ* on strips of Sylgard (RS Ltd., Corby, Northamptonshire, UK) and fixed overnight in 2.5% (v/v) gluteraldehyde, 2.5% (m/v) paraformaldehyde in 100 mmol l^{-1} phosphate buffer at 4°C, pH 7.4. Samples were processed for electron microscopy as previously described (Johnston et al., 1995).

Antibody preparation

Paired box protein 7 (pax 7) is a transcription factor that can be used as a marker of myogenic progenitor cells (Seale et al., 2000). A full-length *pax 7* cDNA was isolated from the fast muscle of the LB morph by RT-PCR and 5′RACE, cloned and sequenced as previously described (GenBank; Accession numbers AJ634763-AJ634775; D. Sibthorpe, R. Sturlaugsdóttir, B. K. Kristjansson, H. Thorarensen, S. Skúlason and I. A. Johnston, manuscript submitted). Zebrafish *pax 7* exonic sequences were aligned with the Arctic charr *pax 7* sequence to delineate exon/intron borders. Pattern searching of protein sequences was performed using the PROSITE database. A 13-amino-acid peptide was identified in the C-terminal region that was conserved among fish and with mouse and was specific to the Pax 7 protein. The peptide, H-Gly-Asp-His-Ser-Ala-Val-Leu-Gly-Leu-Leu-Gln-Val-Glu-NH_2, was commercially synthesised, conjugated to keyhole limpet haemocyanin, and used to immunise two rabbits to provide antisera (Cambridge Research Biochemicals Ltd, Cleveland, UK).

Other antibodies

Polyclonal antibodies were prepared against peptide antigens designed from the Atlantic salmon *Salmo salar* L. *MyoD1* sequence (S. Gottenspare, T. Hansen and I. A. Johnston, unpublished), the Tiger pufferfish *Takifugu rubripes*, Forkhead Protein K1-α (FoxK1-α) previously called Myocyte Nuclear Factor-α) sequence (J. O. Fernandes, and I. A. Johnston, unpublished) and the common carp *Cyprinus carpio* L. Myf-5 sequence (C. M. Martin and I. A. Johnston, unpublished). FoxK1-α is a winged-helix transcription factor that is expressed in activated MPCs (Bassel-Duby et al., 1994), whereas MyoD and Myf-5 are members of the MyoD family of Myogenic Regulatory Factors involved in muscle lineage specification (Rudnicki and Jaenisch, 1995). S58 was obtained from the Developmental Studies Hybridoma Bank, University of Iowa. S-58 is a mouse IgA monoclonal antibody against chicken slow muscle myosin (Crow and Stockdale, 1968) that cross-reacts with slow muscle myosin in several teleost species (Devoto et al., 1996; Johnston et al., 2003a).

Immunohistochemistry

Frozen sections were fixed in acetone for 10 min and air dried for 10 min. Myogenic progenitor cells (MPCs) were identified using primary antibodies to Pax 7, Foxk1-α, Myf-5 and MyoD. Slow muscle fibres were identified using the S-58 antibody. Serial sections were used for single antibody staining.

Primary antibodies were diluted in PST: 1% (v/v) Triton X-100, 1.5% (m/v) BSA (bovine serum albumin) in PBS (phosphate-buffered saline) as follows: S58 1:10 (v/v), Pax-7 1:2000 (v/v), MNF-α 1:1000 (v/v), MyoD and Myf-5 1:800 (v/v). Anti-mouse IgA–biotin conjugate (Sigma, Poole, UK) and anti-rabbit IgG–biotin conjugate (Sigma) secondary antibodies were diluted 1:20 (v/v) and 1:800 (v/v) in PST. PST was also used as a dilutent for blocking and the ExtrAvidin-Peroxidase (Sigma) step. PBS (Sigma) was used for all washes. Sections were blocked in 5% (v/v) normal goat serum (Sigma) for 1 h, washed in PBS for 5 min and incubated overnight at 4°C in the primary antibody. After 3× for 3 min washes the sections were then incubated in the appropriate secondary antibody for 1 h at room temperature, washed again for 3× 3min and incubated in 1:20 (v/v) ExtrAvidin-Peroxidase for 30 min. The sections were washed 3× for 3 min in PBS and developed using 3-amino-9-ethylcarbazole (Sigma), which produces an insoluble red end product. The reaction was terminated by washing with distilled water and the slides were mounted using glycerol gelatine (Sigma).

Determination of the density of MPCs and myonuclei in tissue sections

The density of myonuclei and mononuclear cells stained with Pax 7, FoxK1-α, MyoD and Myf-5 was determined at a magnification of 40× in 25–40 fields of 0.1 mm^2 in each of two blocks where available (for small fish one block contained the entire trunk cross-section). The average diameter of 12 nuclei from mononuclear cells was determined from transmission electron micrographs at a magnification of 19 000 times. Nuclear counts were corrected for section thickness and the mean diameter of nuclei (Abercrombie, 1946).

Nuclear content of isolated muscle fibres

Small bundles of fast muscle fibres were isolated from the dorsal myotome immediately behind the region sampled for histology. Fibre bundles were pinned at their resting length on strips of Sylgard (RS Ltd.) and fixed for 6–10 h in 4% (m/v) paraformaldehyde, PBS. Single muscle fibres freed from connective tissue were isolated in PBS solution using a binocular microscope fitted with dark field illumination. Fibres were suspended in 1% (m/v) saponin in PBS for 3 h, washed three times in PBS and treated with 2 μg ml^{-1} units RNAase (Sigma Chemical, Poole, Dorset). Following further washes in PBS the nuclei were stained with 30 μmol l^{-1} l^{-1} SYTOX green® (Molecular Probes Inc, Leiden, The Netherlands) in PBS for 5 min in the dark. Fibres were mounted on glass slides using fluorescent mounting medium (DAKO Corp., Carpinteria, CA, USA) and viewed using a laser confocal microscope (BioRad Radiance 2000; Hemel Hempstead, Hertfordshire, UK). The number of fluorescent myonuclei was

quantified in fibre segments of 0.3–0.6 mm using a *z*-series of 1 μm optical thick sections and LaserPix *vs* 4.0 software (BioRad, Hemel Hempstead, UK).

Muscle cellularity

S-58 stained sections counterstained with Haematoxyolin were used to determine muscle cellularity. The cross-sectional areas of a minimum of 600 slow and 1000 fast muscle fibres were measured per fish, sampled equally between the blocks and the equivalent fibre diameter computed. The total number of muscle fibres per trunk cross section was estimated as previously described (Johnston et al., 1999). Nonparametric statistical techniques were used to fit smoothed probability density functions (pdfs) to the measured diameters using a kernel function as described in Bowman and Azzalini (1997). The application of these methods to the analysis of muscle fibre diameters has been described in detail previously (Johnston et al., 1999). Values for the smoothing parameter *h* (Bowman and Azzalini, 1997) were in the range 0.055 to 0.103 with no systematic variation between morphs. Muscle fibre recruitment was estimated to have stopped when no fibres in the smallest size class, 4–10 μm diameter were present. The final number of fast muscle fibres (FN_{max}) was the mean ± S.E.M. of the fibre number estimate for all the fish in which fibre recruitment had stopped. The 97th percentile of fibre diameter, calculated from the smooth distributions, was used as an estimate of the maximum fibre diameter (D_{max}).

Statistical analysis

The data were tested for equal variance and normality. Values for D_{max} and FN_{max} were analysed using a GML-ANOVA (general linear models-analysis of variance) with morph as a fixed factor and with either the total cross-sectional area of muscle, fork length or body mass as a covariate (MinitabTM statistical software; Minitab Inc., State College, USA).

Results

Characteristics of the morphs

More than 2000 fish were caught in Thingvallavatn over the 3 years of this study, of which 114 were selected for the analysis of muscle cellularity, covering the body size range of each morph. DB morphs of 7–8 cm fork length, age 2–4 years, were caught containing 8–12 ripe eggs whereas the smallest ripe females of the large benthic and piscivorous morphs captured were 25–30 cm fork length and 7–9 years old. The smallest female planktonic morph with ripe eggs was 19.4 cm. The maximum size of the dwarf morph caught was 25–27 cm compared to 48.5 cm for the large benthic morph and 55.8 cm for the piscivorous morph. The maximum size of each morph captured equalled or exceeded that reported in previous studies (Skúlason et al., 1996).

Muscle fibre types

The composition of myotomal muscle fibres in early life stages was investigated in the progeny of DB, LB and PL morphs reared in the laboratory. At hatching, the myotome largely consisted of fast fibres that were unstained by the S58 antibody (Fig. 2A), and stained weakly for glycogen and succinic dehydrogenase (SDHase) activity (not illustrated). There was a superficial, 1–2 fibre thick, layer of muscle that was highly stained for SDHase and glycogen, which extended from the midline along the whole lateral surface of the myotome (not illustrated). The superficial fibres at the mid-line stained intensely with the S58 antibody (s-s in Fig. 2A) whereas those in the dorsal and ventral regions of the myotome (s-u in Fig. 2A) were weakly stained or unstained. Following first feeding, and through the juvenile stages, all the superficial fibres stained with S58 except for a small number beneath the skin close to the major horizontal septum. This is illustrated for a 4.5 cm DB morph in Fig. 2B, in which the fibres unstained with S58 are labelled with arrowheads. In fish greater than 7.0 cm *FL*, all the superficial muscle fibres stained with S58 (Fig. 2C). The S58^{+ve} fibres stained much more intensely for glycogen (Fig. 2D) and SDHase (Fig. 2E) than the unstained fibres. Myosin ATPase staining following 1 min preincubation at pH 4.3 (Fig. 2F) or pH 10.4 (not illustrated) revealed two fibre types. Fibres lightly stained for myosin ATPase stained intensely for S58 and corresponded to slow fibres whereas fibres unstained by S58 were darkly stained for myosin ATPase, and corresponded to fast fibres (Johnston et al., 1975). Although the superficial fibres had a slightly higher level of staining for glycogen (Fig. 2D) and SDHase (Fig. 2E) than the deeper fibres they were not differentiated on the basis of either S58 or myosin ATPase activity. Following 90–120 s preincubation at pH 4.3 the fast muscle showed a mosaic pattern of staining for myosin ATPase, comprising large darkly staining and small lightly staining fibres (Fig. 2G). This probably represents growth stages of fast fibres rather than the presence of distinct fibre types, reflecting the different composition of fast myosin heavy chain isoforms in large and small diameter fibres documented previously (Ennion et al., 1999). Arctic charr probably have just two main fibre types, based on contractile protein properties. There were no obvious differences in the composition or relative amounts of different muscle fibre types in the DB, LB and PL morphs between hatching and the early juvenile stage.

Muscle fibre recruitment

The production or recruitment of slow muscle fibres was continuous with increasing fork length, and fibre number scaled with body mass $M_b^{0.45}$, with no significant difference between morphs (Fig. 3). Slow muscle fibres with diameters in the range 4–10 μm were surprisingly rare given the steady increase in slow fibre number with increasing body length/mass. In juveniles (<10 cm *FL*), a layer of newly recruited slow fibres was sometimes observed adjacent to the fast muscle layer at the major horizontal septum (arrowheads in Fig. 4A), consistent with a discrete germinal zone as described previously for stratified hyperplasia (Rowlerson and Veggetti, 2001). However, isolated small diameter fibres could

be observed in all regions of the slow muscle and in all stages examined, including the largest piscivorous morph examined (Fig. 4B–D). It was concluded that recruitment of slow fibres continued throughout growth.

The main method of fibre expansion in the fast muscle was mosaic hyperplasia. In mosaic hyperplasia, myotubes form on the surface of existing muscle fibres and mature into small muscle fibres in the size class 4–10 μm. To investigate muscle fibre recruitment in the different morphs, smooth distributions were fitted to measurements of 1000 fibres per individual using a nonparametric Kernel function (illustrated for the DB morph in Fig. 5A; the insert shows an expanded view of the left-hand side of the distribution). The broken lines represent the probability density functions (pdfs) of fibre diameter for individual fish. A total of eight fish, all >18.5 cm *FL*, had no fibres in the size class 4–10 μm and were considered to have stopped myotube production (red lines in Fig. 5A). The median fibre diameter increased, and the right-hand tail of the distribution progressively moved to the right as fork length increased. The blue line represents the probability density function of fibre diameter in the largest DB morph of 27.1 cm *F*L. Examination of the pdfs of fibre diameter of the other morphs in relation to fork length (not shown) revealed that the recruitment of fast muscle fibres ceased at a clearly defined

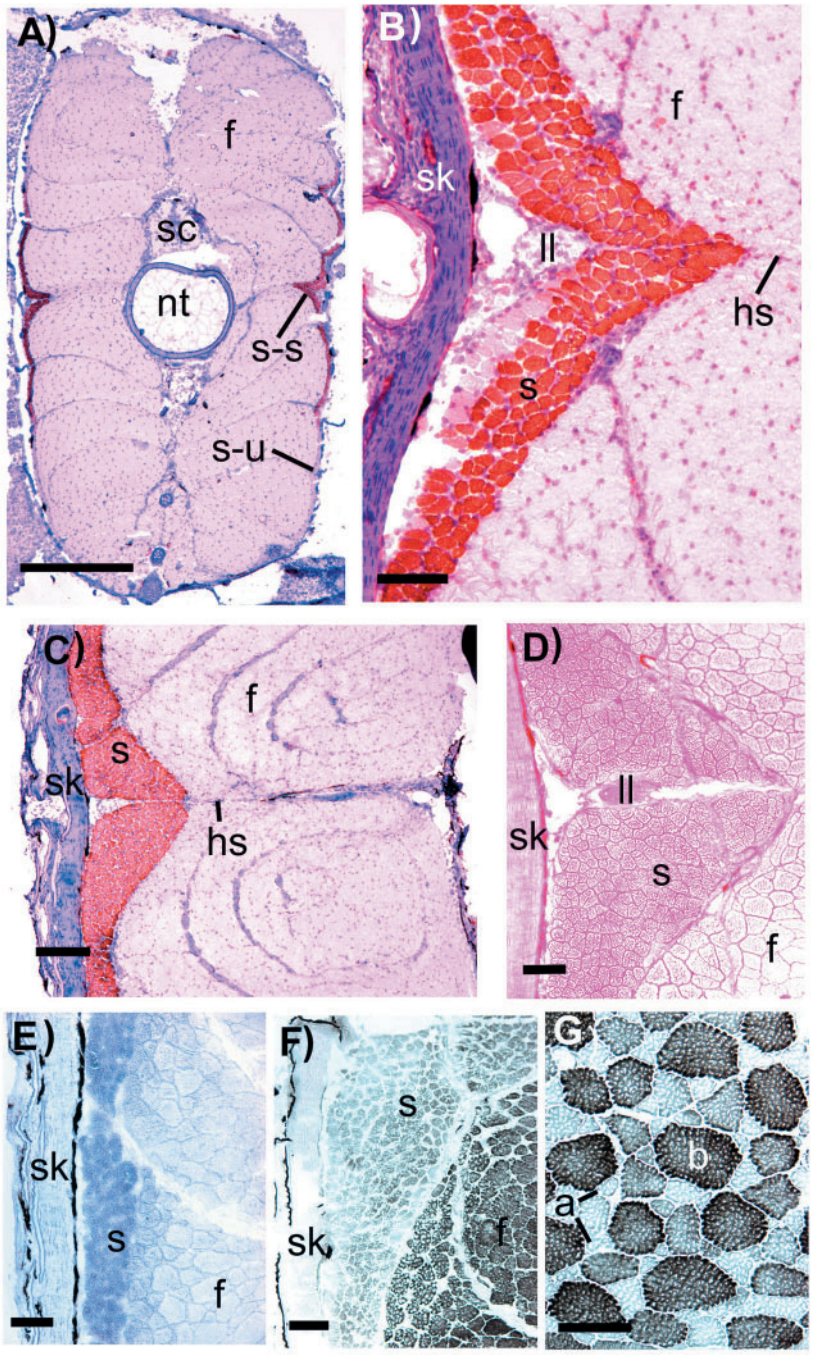

Fig. 2. Muscle fibre types in transverse myotomal sections from juvenile Arctic charr *Salvelinus alpinus* L. (A) A laboratory reared planktivorous morph stained with the S58 anti-slow muscle myosin antibody and counterstained with Haematoxylin–Eosin. Note the superficial layer of fibres darkly stained with S-58 (red) centred on the major horizontal septa (s-s). In contrast, the superficial fibres at the dorsal and ventral surfaces of the myotome are weakly stained or unstained with S-58 (s-u). Scale bar, 500 μm. (B) A wild-caught dwarf benthic morph, 4.5 cm *FL*, stained with S-58 antibody and counterstained with Haematoxylin. The majority of the slow fibres (s) stained intensely for S-58 whereas a small number of the slow fibres (arrowhead) and the fast fibres (f) were unstained. Scale bar, 100 μm. (C) A wild-caught dwarf benthic morph, 5.5 cm *FL*, stained with S-58 antibody and counterstained with Haematoxylin–Eosin. Note that at this body length all the slow fibres (s) stained with S-58. There was no evidence for fibres showing intermediate expression for the antigen to S-58 between the slow (s) and fast (f) muscle layers. Scale bar, 200 μm. (D) A wild-caught dwarf benthic morph, 8.4 cm *FL*, stained for glycogen. The slow fibres (s) were more intensely stained (magenta) than the fast fibres (f). Scale bar, 100 μm. (E,F) A wild-caught dwarf benthic morph, 8.4 cm *FL*. (E) Epaxial region of the myotome stained for succinic dehydrogenase (SDHase) activity (blue staining). Slow fibres (s) stained intensely for SDHase whereas fast fibres (f) were weakly stained. (F) Region hypaxial to the major horizontal septum stained for myosin ATPase activity following 1 min preincubation at pH 4.3. The slow fibres (s) were lightly stained and the fast fibres (f) were darkly stained. Scale bars, 100 μm. (G) The fast muscle of a wild-caught dwarf benthic morph, 9.7 cm *FL*, stained for myosin ATPase activity following 90 s preincubation at pH 4.3. Note myosin ATPase had been inactivated in the immature small diameter fibres (a) but not in the larger diameter fibres (b). Shorter periods of preincubation resulted in uniform dark staining whereas longer periods inactivated the myosin ATPase activity in all diameters of fibres. Scale bar, 100 μm. hs, major horizontal septum; nt, notochord; ll, lateral line nerve; sc, spinal cord; sk, skin.

body length, which was characteristic of each morph. The results of this analysis are summarised in Fig. 5B, which shows that muscle fibre recruitment was complete at 18–19 cm *FL* in the dwarf benthic morph, 33-34 cm in the large benthic morph, 24–26 cm in the planktivorous morph, and 34–35 cm in the piscivorous morph. The fast muscle in a 25.7 cm *FL* DB morph, which stopped recruiting fibres at ~18 cm, is illustrated in Fig. 6A. Note the absence of fibres less than 30 μm. In contrast, a PI morph at 35.8 cm *FL* still contained fibres in the size range 10–14 μm reflecting the longer duration of fibre recruitment with respect to length in this morph (Fig. 6B). Thus at a given *FL* the distribution of fibre diameters differed between morphs reflecting the different durations of fibre recruitment with respect to length. The largest DB morph of 27.1 cm had no fast fibres smaller than 45 μm diameter, a situation that was not reached in the PI morph until 50.1 cm *FL* (not illustrated).

The relationship between the number of fast muscle fibres and body length for each morph is shown in Fig. 7. For presentational purposes the data were organised into bins of increasing body size and average values and multidirectional error bars were calculated. An ANOVA with morph as a fixed factor revealed significant differences in fibre number with either *FL* ($F_{3,110}$=9.62; P<0.001) or total muscle cross-

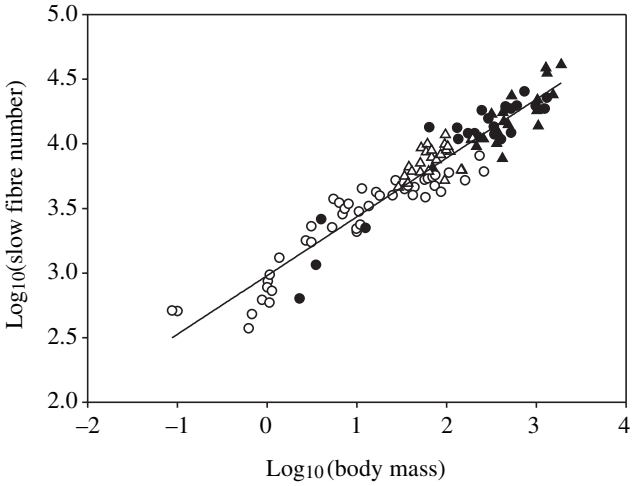

Fig. 3. A double logarithmic plot of the number of slow muscle fibres per myotomal cross-section at 0.7 *FL* and M_b in Arctic charr from Thingvallavatn. The data points represent dwarf benthic morphs (open circles), planktivorous morphs (open triangles, large benthic morphs (filled circles) and piscivorous morphs (filled triangles). A first order polynomial was fitted to the data with the following equation: $\log_{10}$(slow fibre number)=$\log_{10}$2.98±0.027+ 0.45±0.114($\log_{10}FL$) (r^2=0.91; d.f. 112; ANOVA; $F_{1,111}$=1134.4; P<0.0001).

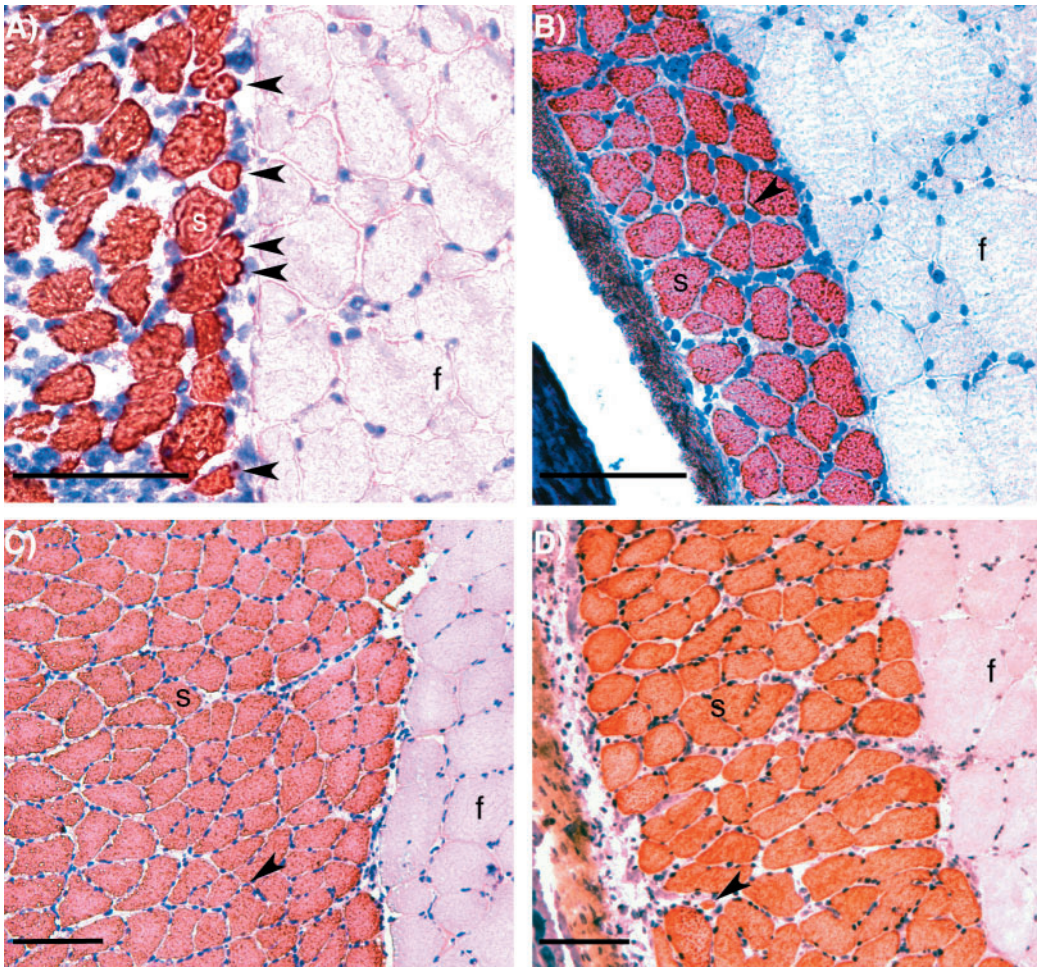

Fig. 4. Transverse sections of myotomal muscle from wild-caught Arctic charr *Salvelinus alpinus* from Thingvallavatn. All sections were stained with the S-58 anti-slow muscle myosin antibody and counterstained with Haematoxylin. The slow muscle fibres (s) stain red and the fast muscle fibres (f) are unstained. (A) Large benthic morph, 8.0 cm *FL*. The arrowheads show a zone of small diameter slow fibres adjacent to the fast muscle layer representing a region of stratified hyperplasia. (B) Planktiverous morph, 20.6 cm *FL*. The arrowhead shows an isolated small diameter fibre within the slow muscle layer. (C,D). Piscivorous morphs, 35.8 cm *FL* (C) and 50.6 cm (D). The arrowheads show an isolated small diameter fibre within the slow muscle layer. All scale bars, 100 μm. f, fast muscle fibre; s, slow muscle fibre.

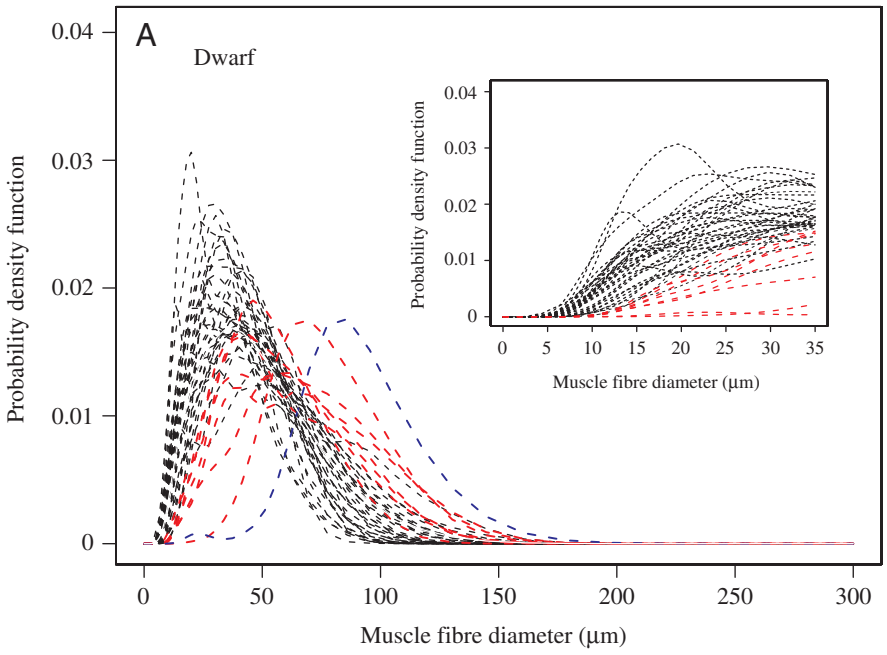

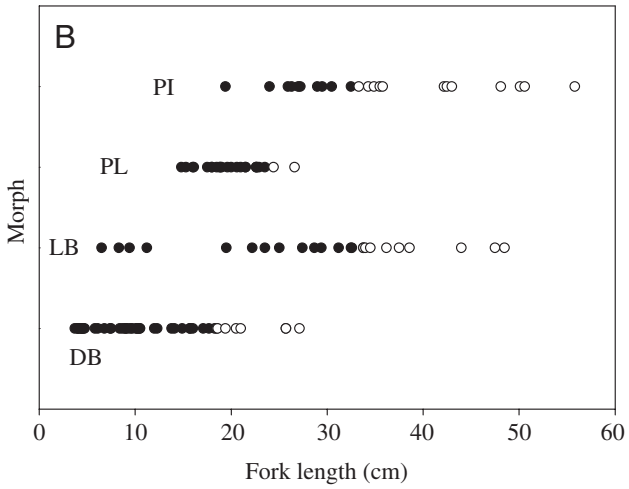

Fig. 5. (A) The distribution of fibre diameters in the fast myotomal muscle for 46 dwarf benthic morphs ranging in size from 3.7 cm to 27.1 cm *FL*. Smooth nonparametric distributions were fitted to measurements of a minimum of 1000 fibre diameters per fish using a kernel function (see text for details). The insert shows the detail of the left-hand side of the distribution. The probability density functions of fish containing fibres in the 4–10 μm size category are shown in black (broken lines). Fish with no fibres in this size category that were considered to have stopped recruiting fibres are shown in red. The blue broken lines represent the largest fish examined (27.1 cm *FL*). (B) A diagrammatic representation of the entire data set showing the presence (closed circles) and absence (open circles) of muscle fast fibres less than 10 μm in relation to fish fork length for the dwarf benthic (DB), large benthic (LB), planktivorous (PL) and piscivorous (PI) morphs.

sectional area ($F_{3,110}$=17.64; P<0.001) as covariates. The maximum fibre number (FN_{max}) in each of the morphs is shown in Table 1. Since there was no significant difference between FN_{max} for the LB and PI morphs the data were combined. FN_{max} in the DB morph was 56.5% of the value found in the LB and PI morphs combined (P<0.001; one-way ANOVA; Table 1). The data on the largest planktivorous morphs was limited, with the two largest fish of 24 and 26 cm *FL* having stopped recruiting fibres, consistent with a difference between the PL and PI/LB morphs (Table 1). For individuals showing active muscle fibre recruitment, fibre number scaled with $M_b^{0.51}$ in the DB and PL morphs combined, and $M_b^{0.31}$ in the LB and PI morphs combined (P<0.01; Fig. 8).

A 3-D plot of the relationship between the number of fast muscle fibres in the DB, LB and PI morphs, fork length and age is shown in Fig. 9. The individual fish that have stopped recruiting fast muscle fibres are identified by coloured symbols. The youngest fish that had ended recruitment was a 4+ year class individual in the case of the DB morph, and 7+ year class individuals in the case of the LB and PI morphs (Fig. 9). The cessation of fibre recruitment coincided with a threshold body length and occurred over a range of ages (Fig. 9). Thus, a 9+ year class DB-morph, a 12+ year class LB-morph and a 14+ year class PI morph were caught that were below the threshold fork length and these individuals were still producing fast muscle fibres.

Muscle fibre hypertrophy

The maximum diameter (D_{max}) of each fibre type was estimated by calculating the 97th percentile of fibre diameter for each fish from the smooth distributions of fibre diameter. For fish greater than M_b=10 g, a linear relationship between $\log_{10}D_{max}$ and $\log_{10}M_b$ was observed for both fibre types (Fig. 10). The mass exponent was 0.18, and no significant difference was observed between morphs. Fish weighing less than 10 g had a maximum fibre diameter considerable greater than predicted by these scaling relationships (not illustrated).

Fibre myonuclei content

The distribution of nuclei in representative isolated single slow and fast muscle fibre segments is illustrated in Fig. 11A,B. The majority of nuclei in the confocal images were found in planes of focus corresponding to the sub-sarcolemmal zone. The myonuclei content of fibres for any given diameter was significantly higher for slow than fast muscle fibres ($F_{1,878}$=3968.0; P<0.0001). The relationship between myonuclei content and fibre diameter is illustrated in Fig. 11C. Second order polynomials were fitted to the data (Fig. 11C). For fibres of 60 μm diameter, the myonuclei contents calculated from the regressions were twofold higher for slow

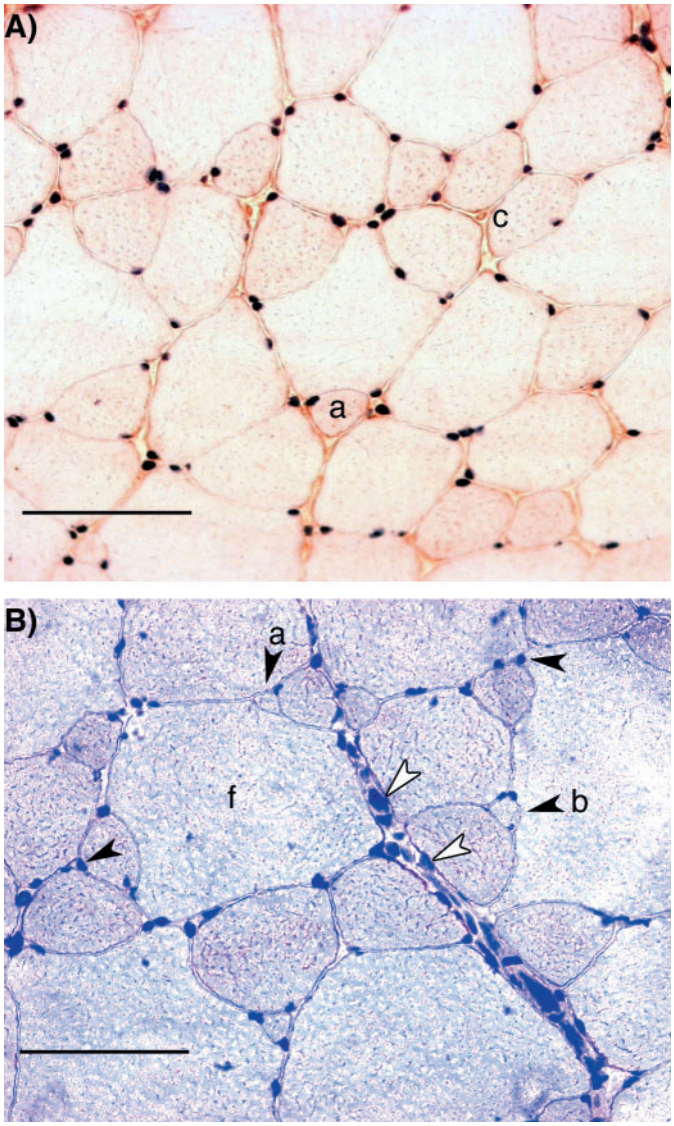

Fig. 6. Transverse sections of fast myotomal muscle from Arctic charr stained with S-58 antibody and counterstained with Haematoxylin–Eosin. (A). Dwarf benthic morph, 25.7 cm *FL*, showing the absence of fast muscle fibres less than 20 μm diameter. The smallest diameter fibre is labelled (a). (B) Piscivorous morph, 35.8 cm *FL*, showing the mosaic pattern of muscle fibre diameters indicating recent recruitment. The fibres labelled (a) and (b) are 14 and 18 μm diameter, respectively. Filled arrowheads, muscle nuclei; unfilled arrowheads, connective tissue nuclei. Scale bars, 100 μm. c, capillary.

muscle fibres (2264 nuclei cm^{-1}) than for fast muscle fibres (1126 nuclei cm^{-1}).

Myogenic progenitor cell density

Myogenic progenitor cells (MPCs) were identified using a specific antibody to Pax 7 (Fig. 12A). Those MPCs that were committed to differentiation were identified using antibodies to Fork head protein K1-α (FoxK1-α; Fig. 12B), MyoD and Myf-5 (not illustrated). MPCs immunoreactive to the myogenic regulatory factor Myf-5 were also quantified. The density of myonuclei (Fig. 13A) and the density of Pax 7 immunoreactive cells (Fig. 13B) decreased with increasing fork length. However, in the case of Pax 7, FL only accounted for 17% of the total variation (Fig. 13B). The density of cells immunopositive for the other transcription factors investigated was similar over the length range 18–48 cm (Fig. 14A–C). The average density of cells staining for phenotypic markers of MPCs as a percentage of total myonuclei density was 3.2% for Pax 7, 2.8% for FoxK1-α, 1.9% for MyoD and 1.7% for Myf-5.

Table 1. *The maximum number of fast muscle fibres* (FN_{max}) *in Arctic charr morphs from Thingvallavatn*

Morph	Number of fish	FN_{max}
Dwarf benthic (DB)	8	$6.97\times10^4\pm4.22\times10^3$
Large benthic (LB)	8	$1.14\times10^5\pm3.10\times10^3$
Planktivorous (PL)	2	9.15×10^4
Piscivorous (PI)	12	$1.30\times10^5\pm4.96\times10^3$
LB and PI combined	20	$1.23\times10^5\pm3.63\times10^3$ ***

Values represent means ± S.E.M.

***Significant difference from the DB morph at the $P<0.001$ level (one-way ANOVA).

Rearing experiments

Embryos from the large benthic, pelagic and dwarf benthic morphs were incubated under two temperature regimes designed to simulate groundwater-fed spawning sites (2.2–3.2°C) and the general lake temperature (September–April) (4–7°C). None of the progeny of DB morphs incubated at the higher temperature survived until hatching. The $\log_{10}$(fast fibre number) plotted against *FL* for fish between hatching and 2–3 weeks after first feeding is illustrated in Fig. 15A. An ANOVA with morph and temperature regime as fixed factors revealed no significant differences between rearing regimes. A linear regression equation, with a slope of 0.19 ± 0.017 and an intercept of 2.98 ± 0.051, was fitted to the data (Fig. 14A; $F_{1,51}=125.1$; $P<0.0001$). The average fibre diameter also showed no significant differences with rearing temperature (Fig. 15B). The density of cells immunopositive for Pax 7, FoxK1-α, MyoD and Myf-5 in the offspring of LB and PL morphs is illustrated in Fig. 16A–C. An ANOVA with rearing temperature and morph as fixed factors revealed no significant differences between groups. The density of cells expressing these MPC markers was generally higher than in larger fish (see Figs 12, 13).

Discussion

Patterns of muscle fibre recruitment

Few other studies have investigated the recruitment of both slow and fast myotomal fibres over the complete size range of

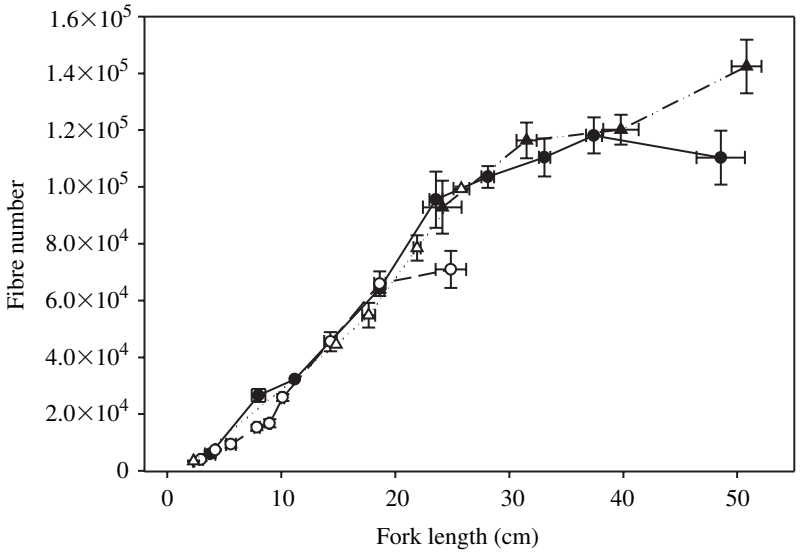

Fig. 7. The relationship between fork length (*FL*) and the number of fast muscle fibres per trunk cross-section in the DB morph (open circles), the LB morph (filled circles), the PL morph (open triangles) and the PI morph (filled circles). The bidirectional error bars represent means ± S.E.M. Fish of a similar size were grouped together in order to show the differences between morphs more clearly. The numbers of fish in each size bin in order of increasing fork length were as follows: LB: 4, 5, 5, 5, 4; DB: 10, 7, 6, 8, 7, 4, 4; PL: 8, 8, 8; PL: 6, 4, 8, 4.

a teleost species. The present study revealed a continuous recruitment of slow muscle fibres in all morphs of Arctic charr, and that slow fibre number scaled to $M_b^{0.45}$ (Fig. 3). Similarly, slow fibre number was reported to increase with body length in the zebrafish, a species that only reaches 5–6 cm when fully grown (Van Raamsdonk et al., 1983). In contrast, most studies have shown that the recruitment of fast muscle fibres continues until a defined body length, after which growth is entirely by the hypertrophy of fibres formed earlier in development (Weatherley et al., 1980, 1988; Stickland, 1983; Johnston et al., 2000c, 2003a,c,d). Postembryonic myogenesis therefore differed between slow and fast muscles with respect to the duration of fibre recruitment. Skeletal muscle fibres are post-mitotic and growth involves a population of myogenic progenitor cells (MPCs) that retain the ability to divide. In mammals, there is considerable evidence for heterogeneity in the MPCs from different muscle types in adult stages (Feldman and Stockdale, 1991; Hawke and Garry, 2001; Levin et al., 2001; Mootoosamy and Dietrich, 2002; Tajbakhsh, 2003). For example, MPCs isolated from adult rabbit fast- and slow-twitch muscle differentially express the secreted frizzle-related protein thought to be involved in cell fate determination (Levin et al., 2001). The embryological origin

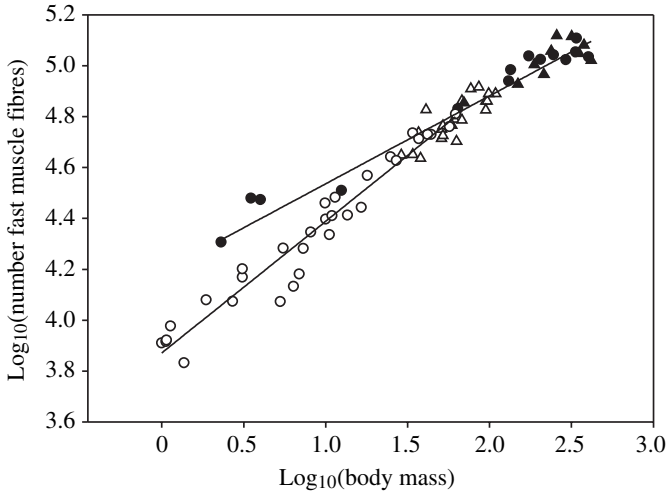

Fig. 8 Double logarithmic plots of fibre number and body mass for those fish actively producing muscle fibres. Symbols as for Fig. 7. First order polynomials were fitted to the data for the DB and PL morphs combined and the LB and PI morphs combined, which had the following equations. DB+PL morphs: $\log_{10}$(fibre number)=$\log_{10}$3.88±0.020+$\log_{10}$(M_b)0.52±0.014 (r^2=0.96; d.f.=51; P<0.0001). LB+PI morphs: $\log_{10}$(fibre number)=$\log_{10}$4.24±0.031+$\log_{10}$(M_b)0.33±0.015 (r^2=0.96; d.f.=51; P<0.0001). Values are means ± S.E.M.

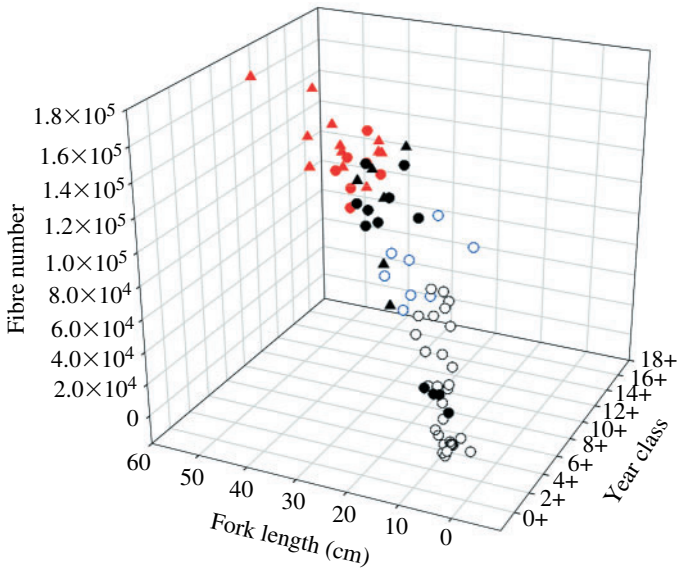

Fig. 9. A 3-D plot of the number of muscle fibres in Arctic charr morphs *vs* fork length and year class. DB morphs (open circles), LB morphs (filled circles) and PI morphs (filled triangles). The coloured symbols represent individuals that had stopped recruiting muscle fibres.

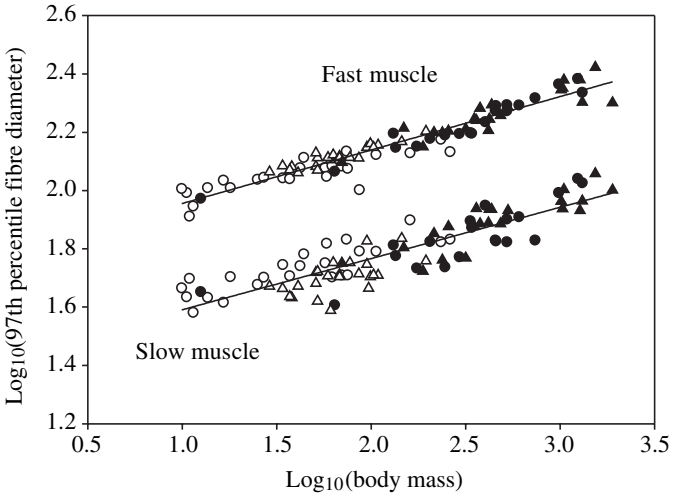

Fig. 10. A double logarithmic plot of the 97th percentile of fibre diameter calculated from the smoothed distributions of fibre diameter (see text) and body mass for the DB morph (open circles), the LB morph (filled circles), the PL morph (open triangles) and the PI morph (filled triangles) of Arctic charr. First order polynomials were fitted to the data for fish greater than 10 g body mass. The relationships in slow and fast muscle are illustrated and the parameters for the equations were as follows. Fast muscle: intercept=$\log_{10}$1.77±0.013; slope=0.18±0.0060 (r^2=0.92; ANOVA $r^2_{1,88}$=948.4; P<0.0001). Slow muscle: intercept=$\log_{10}$1.42±0.022; slope=0.18±0.010; (r^2=0.77; ANOVA $F_{1,88}$=297.9; P<0.0001).

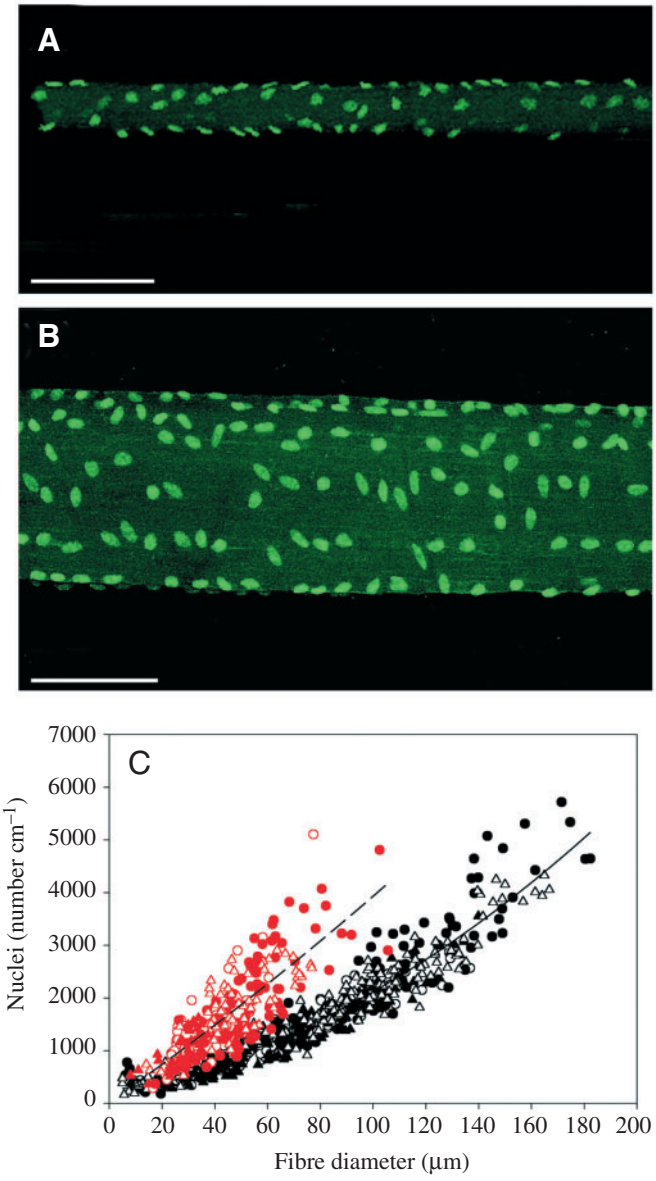

Fig. 11. The myonuclei content of isolated single fibres from (A) a slow muscle fibre 27 μm in diameter and (B) a fast muscle fibre 157 μm in diameter. The images represent a computed reconstruction of a *z*-series of 1 μm confocal sections through the fibre. The nuclei (green) were visualised by staining with SYTOX green®. (C) The relationship between muscle fibre diameter (μm) and the number of nuclei per cm in single fibre segments isolated from the slow (red symbols) and fast (black symbols) myotomal muscle from the DB morph (open circles), the LB-morph (filled circles), the PL morph (open triangles) and the PI morph (filled triangles). Fibres were isolated from 4–6 individuals per morph in the size range 20–27 cm *FL*. The fitted lines represent second order polynomials with the following equations. Slow muscle: nuclei cm^{-1}=23.38+34.76 (fibre diameter)+0.043(fibre diameter)^2 (Adj. r^2=0.65; residual d.f.=247; P<0.0001). Fast muscle: nuclei cm^{-1}=231.80+9.00 (fibre diameter)+0.098 (fibre diameter)^2 (Adj. r^2=0.92; residual d.f.=620; P<0.0001).

and the phenotypes of MPCs in teleost fast and slow muscles are important questions for future research.

The major finding of the present study was that the recruitment of fast muscle fibres in the Arctic charr morphs in Thingvallavatn was related to ultimate body size. Our null hypothesis that the number and size distributions of myotomal muscle was the same in all morphs was therefore rejected for fast muscle. The cessation of muscle fibre recruitment in Arctic charr was related to fork length, not age (Fig. 9), with recruitment stopping at 18 cm for the DB-morph, 24–26 cm for the PL morph and around 33–35 cm for the LB and PI morphs (Figs 5B, 7). During the hyperplastic phase of growth fast fibre number scaled with $M_b^{0.52}$ in the DB and PL morphs and $M_b^{0.33}$ in the LB and PI morphs (Fig. 8). Thus fibre number (*FN*) was lower in juvenile DB than LB morphs, although the increase in *FN* with increasing body mass was proportionally greater (Fig. 8). The cessation of hyperplasia in fast muscle was not related to sex or correlated with the body length at sexual maturity, which was 7–8 cm in the DB morph and 25–30 cm in the LB morph. The size of the DB morph at maturity may be close to the lower limit for gonadal development in salmonids (Myers et al., 1986). The dwarf morph grows more slowly, but matures earlier than the large benthic morph, which reaches a larger ultimate size (Sandlund et al., 1992). The pattern of growth and maturation in Arctic charr morphs in Thingvallavatn is consistent with optimisation theory, which predicts that slow growth at an early age selects for young age at sexual maturity, whereas growth stagnation at an old age selects for late sexual maturity (Schaffer and Elson, 1975). Hyperplasia in fast muscle had stopped in a 4+ year class DB

morph, whereas the youngest LB and PI morphs that had stopped recruiting fibres were the 7+ year-class (Fig. 9). The age at which the threshold length for cessation of hyperplasia was reached occurred over a wide range of ages, such that a 12+ year-class LB morph and a 14+ year-class PI morph were found that were still recruiting fast muscle fibres (Fig. 9).

The origins of different patterns of fibre recruitment

The environmental temperature during early development has been shown to affect the number of muscle fibres produced at each stage of myogenesis in salmonids (Stickland et al., 1988; Johnston et al., 2000b, 2003c) and other teleosts (Ayala et al., 2000; Johnston et al., 1998). Temperature regimes that result in a higher fibre number have been associated with a higher density of myogenic progenitor cells (Johnston et al., 2000a, 2003c). The effect of this developmental plasticity varies with the temperature profile during embryogenesis and can show marked differences between species and between populations of the same species (Johnston et al., 2000a,b; Johnston and Hall, 2004). In Thingvallavatn, spawning sites that are associated with groundwater input have a stable temperature of 2–3°C whereas the temperature in other areas is more seasonally variable (Skúlason et al., 1989a; Sandlund et al., 1992). Both the DB morph and the LB morph spawn in sites affected by subterranean springs and therefore developmental plasticity is unlikely to be an explanation for the differences in fibre number between these morphs. This was confirmed by rearing the progeny of the DB, LB and PL morphs at temperatures that simulated the temperature in groundwater influenced sites and the general lake temperature over the period of embryonic development (September–April; Skúlason et al., 1989a). No evidence was found for developmental plasticity in either MPC density or fibre number in the progeny of Arctic charr from Thingvallavatn (Figs 14A,C, 15A). Furthermore, the juvenile and adult stages of the DB and LB morphs coexist, and both feed on snails and other benthic invertebrates (Sandlund et al., 1992). We

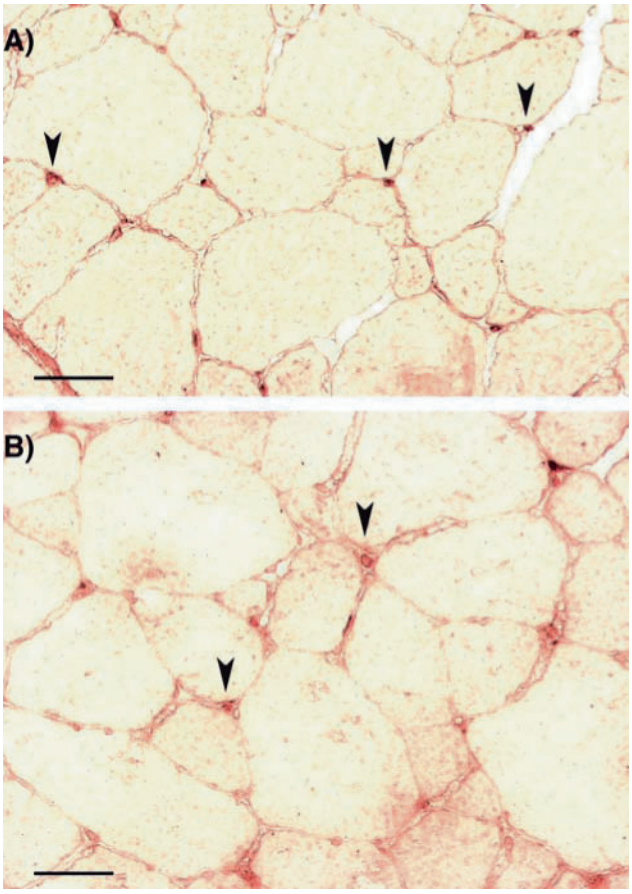

Fig. 12. Immunohistochemistry of molecular markers of myogenic progenitor cells (MPCs) in the fast myotomal muscle of Arctic charr. (A) Pax 7 staining in a transverse section from a piscivorous morph and (B) FoxK1-α staining in a transverse section from a large benthic morph. Arrowheads indicate some of the cells immunopositive for these markers. Scale bars, 50 μm.

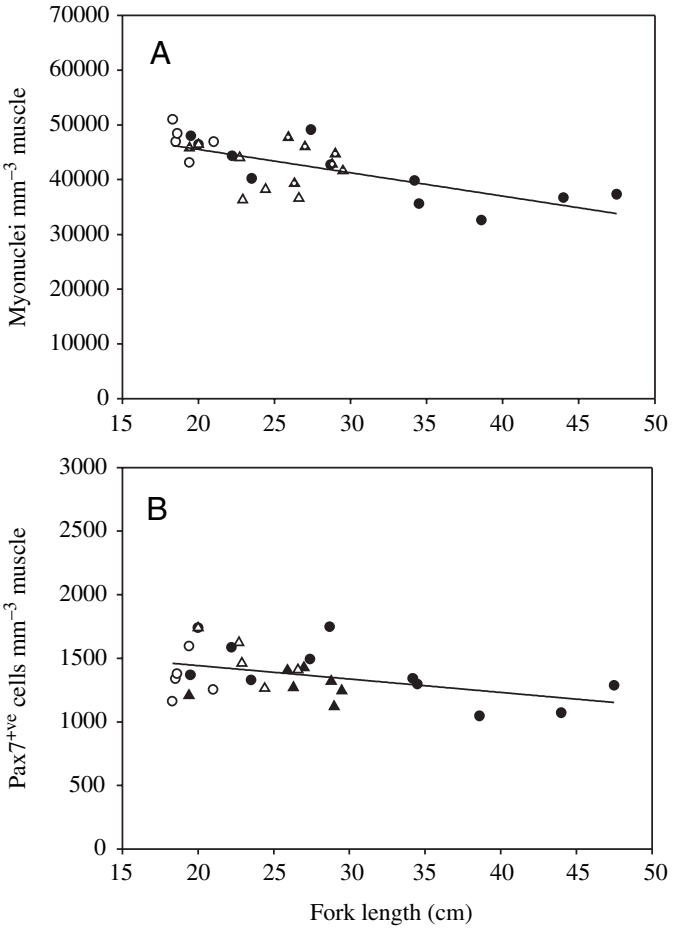

Fig. 13. The relationship between the density (number mm^{-3} muscle) of (A) total myonuclei and (B) Pax 7 immunoreactive cells in tissue sections in relation to fork length for the DB morph (open circles), the LB morph (filled circles), the PL morph (open triangles) and the PI morph (filled triangles). Linear regressions were fitted to the data that had the following equations: density myonuclei= 54029.4–425.8*FL* (r^2=0.45; $F_{1,26}$=21.2; P<0.0001). Density Pax7^{+ve} cells=1653.5–10.54*FL* (r^2=0.17; $F_{1,26}$= 5.44; P<0.05).

therefore conclude that the differences in fibre recruitment patterns between morphs probably have a genetic basis. Consistent with this hypothesis, differences in maximum body size and growth patterns between morphs are maintained in common garden experiments, indicating a large genetic component (Skúlason et al., 1989b, 1993, 1996; Eiríksson et al., 1999).

It has been suggested that in the absence of interspecific competition, pioneer species such as Arctic charr, were subject to intense intraspecific competition for resources, accompanied by character release related to phenotypic plasticity in behaviour and life history (Nordeng, 1983; Skúlason et al., 1999; Snorrason and Skúlason, 2004). Habitat diversity would then be expected to facilitate the diversification of phenotype resulting in discrete resource morphs (Snorrason and Skúlason, 2004). Given sufficient genetic variation, such polymorphisms can be consolidated by genetic selection, and possible mechanisms for the origin of reproductive isolation have been proposed (see Snorrason and Skúlason, 2004). Only the smallest charr would be able to exploit the interstitial spaces of the stony substrate of the lake and size-assortative mating might be expected to promote isolation, restrict gene flow with larger charr and in time lead to the formation of a genetically stable dwarf. There is evidence that such isolation processes can progress very rapidly in the wild in salmonids (Hendry et

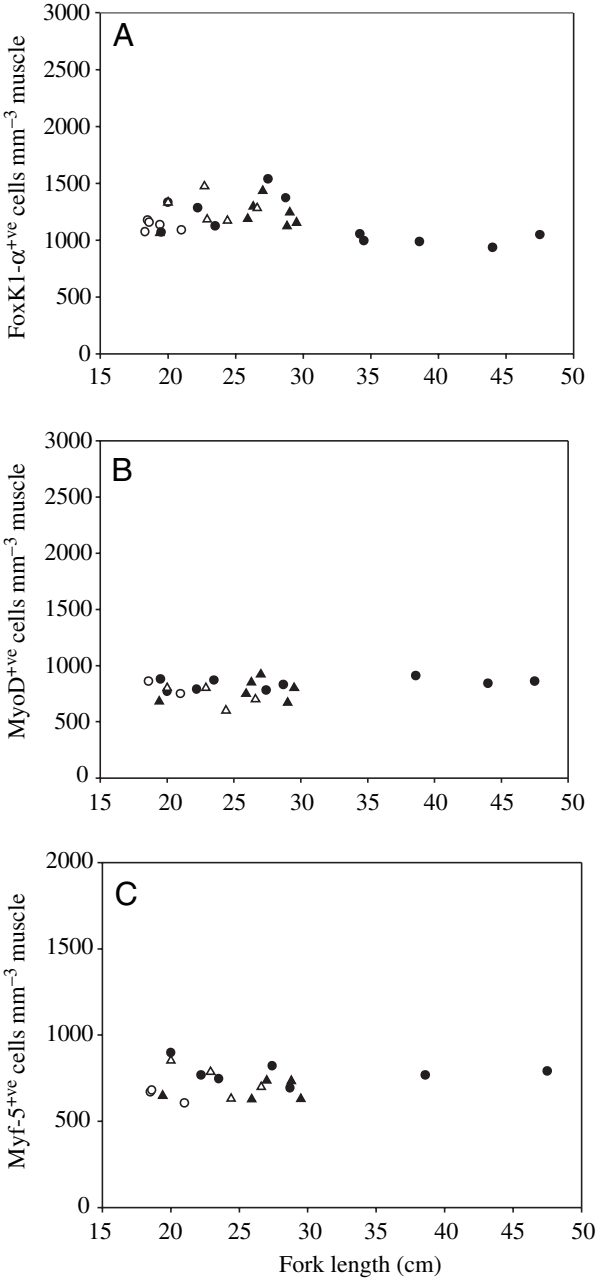

Fig. 14. The relationship between the density (number mm^{-3} muscle) of (A) Forkhead box protein K1-α (FoxK1-α) (B) MyoD and (C) Myf-5 immunoreactive cells in tissue sections in relation to fork length for the DB morph (open circles), the LB morph (filled circles), the PL morph (open triangles) and the PI morph (filled triangles).

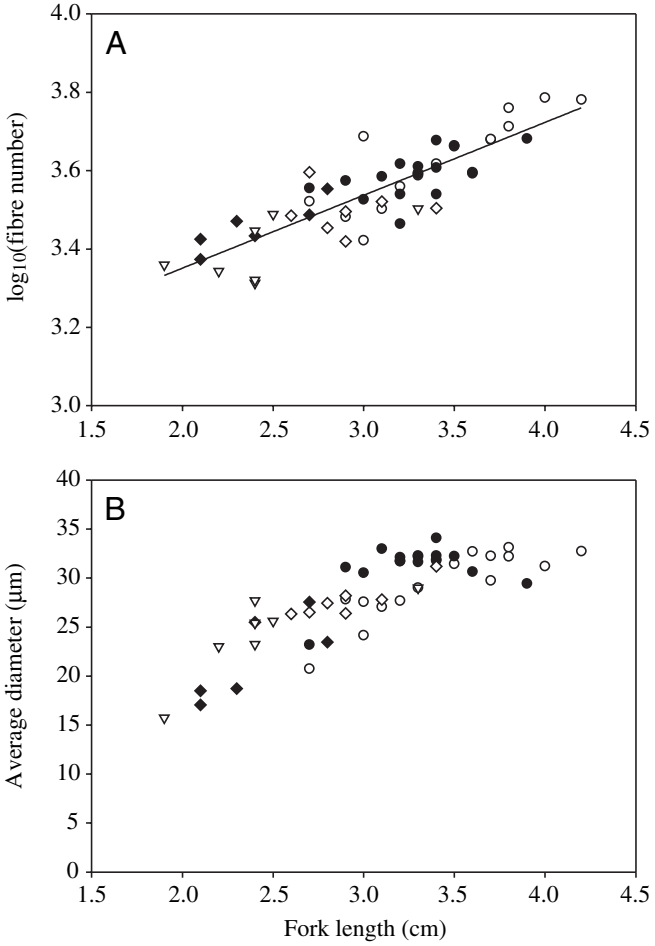

Fig. 15. The influence of rearing temperature on the number and average diameter of fast muscle fibres post-hatch. (A) Log_{10}(fast fibre number per myotomal cross-section) in fry of the dwarf benthic (circles), large benthic (triangles) and pelagic (diamonds) morphs reared at 'cool ambient temperatures' of 2.2–3.2°C (open symbols) or in heated water of 4–7°C (closed symbols). A linear regression was fitted to the data with the following equation: $\log_{10}(\text{fibre number}) = 2.98 + 0.19F$ (r^2=0.71; $F_{1,51}$=125.1; P<0.0001). (B) The average fibre diameter *vs* fork length. Symbols as for A.

al., 2000). The Arctic charr morphs in Thingvallavatn are generally considered to have a sympatric origin (Snorrason et al., 1994; Skúlason et al., 1999), a view supported to varying degrees by data on the genetic structuring of populations within and between lakes (Gíslason et al., 1999; Wilson et al., 2004). An alternative view is that the charr constitute a species complex that evolved allopatrically during the Pleistocene glaciations (Nyman et al., 1981). In either case, the morphs in Thingvallavatn have been diverging for no longer than 10 000 years. Assuming our hypothesis of a genetic explanation is correct then the genes regulating fibre number and the duration of fibre recruitment in fast muscle are under high selection pressure and susceptible to rapid evolutionary change.

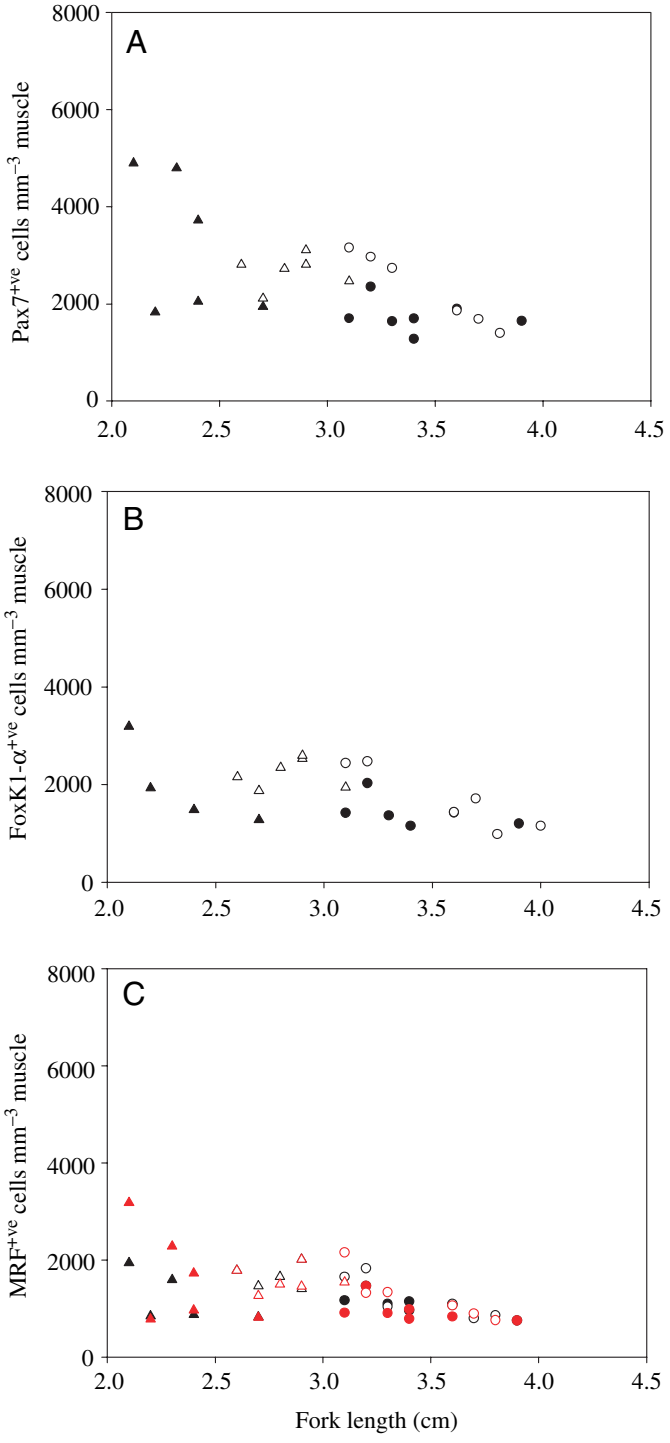

Fig. 16. The relationship between fork length and the density of myogenic progenitor cells staining with antibodies to (A) Pax 7, (B) FoxK1-α and (C) Myogenic Regulatory Factors (black and white symbols represent MyoD and red symbols Myf-5) in the fast muscle of the progeny of PL-morphs (triangles) and LB-morphs (circles) of Arctic charr. The fish were reared at either cold constant temperatures (2.2–3.2°C) or at more variable warmer temperatures (4–7°C).

The optimal fibre size hypothesis

We propose an 'optimal fibre size hypothesis' to explain evolutionary adjustments in muscle fibre number with body size and temperature. The hypothesis requires that there is an optimal maximum fibre diameter, which reflects a trade-off between avoiding diffusional constraints and the need to minimise the costs of ion pumping. Maintenance of ionic homeostasis is thought to constitute 20–40% of the resting metabolic rate in teleosts (Jobling, 1994). The fast myotomal muscle comprises more than 60% of body mass in a typical teleost, and therefore ionic homeostasis in this tissue makes an important contribution to the overall metabolic rate. The surface/volume ratio of muscle fibres decreases with increasing fibre diameter. Thus the surface area for passive membrane leak in large diameter fibres would be expected to be less than for small diameter fibres, and therefore require concomitantly fewer active ion pumps per unit volume in order to maintain ionic equilibria and membrane potential. The Na^+-K^+ pump and the L-type Ca^{2+} pump are probably the most important energy consuming pumps in the muscle sarcolemmal membrane (Clausen, 2003). Important and testable predictions of the hypothesis are that the number of these pumps per unit volume of muscle and their contribution to the oxygen consumption of fibres should decrease with increasing fibre size. Factors such as temperature that change the oxygen concentration at the surface of the muscle fibre and metabolic demand would be expected to shift the optimum diameter and hence the number of muscle fibres required to reach a particular body size. Juvenile and adult Arctic charr in Thingvallavatn live at the same temperature and the similar fibre type proportions and myonuclear content of fibres suggest similar activity patterns. In this case, selection for a small body size in the dwarf morph would have resulted in a concomitant reduction in FN_{max} to produce the optimal trade-off between fibre size and the costs of ionic homeostasis.

Scaling of maximum fibre diameter

For fish greater than 10 g, the maximum diameter was related to M_b by the following equation: $D_{max}=aM_b^b$ where a and b are constants. Double logarithmic plots of D_{max} *vs* M_b gave a scaling coefficient (b) of 0.18 (Fig. 10). Smaller fish contained larger diameter fibres than predicted by the equations in Fig. 10. In the fast muscle, plotting the data for fish between 100 and 1893 g resulted in a slope of 0.22 without a significant decrease in the correlation coefficient. A. V. Hill provided a

solution for the maximum radius (R_O) that oxygen can penetrate in a long circular cylinder of muscle for a given oxygen concentration at its surface (Y_O):

$$R_O = 2(KY_O/V_O)^{1/2}, \quad (1)$$

where K is Krogh's diffusion constant and V_O is the mass specific oxygen consumption of the muscle (Hill, 1965). The mass-specific oxygen consumption at the whole animal level scales with $M_b^{-0.22}$ in salmonids (Clarke and Johnston, 1999). As body size increases the decrease in mass-specific metabolic rate may relax diffusional constraints (i.e. the largest diameter of fibre that is permitted without forming an anoxic core), setting D_{max} at a higher value. Even in the largest fish the diameter of the majority of fibres is much less than D_{max} (Fig. 5A). Therefore somatic growth largely reflects the hypertrophy of fibres that are sub-maximal in diameter.

In vivo the situation is much more complex than described in Equation 1 since the oxygen concentration at the surface of the muscle fibre will depend on the complex geometry of the capillaries supplying the muscle fibres, the perfusion rates of individual capillaries, hematocrit, and the numerous factors influencing the gradient of oxygen between the capillary wall and the mitochondria (Salathe and Gorman, 1997). These factors include the myoglobin concentration, the density of lipid-rich subcellular structures (mitochondria and sarcoplasmic reticulum), and the distribution of the sites of oxygen consumption as well as the metabolic demand (Eggleton et al., 2000; Salathe and Gorman, 1997; Sidell, 1998).

There are several lines of evidence to suggest that diffusion of oxygen limits the maximum diameter of the fast muscle fibres even though contraction is supported from local energy stores and involves anaerobic metabolic pathways. The immediate energy supply for contraction in the fast muscle comes from the hydrolysis of phosphocreatine and is supplemented by anaerobic glycogenolysis during prolonged high-speed swimming, resulting in the accumulation of lactic acid (Hochachka, 1985; Richards et al., 2002). The rate of radial diffusion of a substance is proportional to the reciprocal of the square root of the relative molecular mass, and is much greater for relatively large molecules such as lactate than oxygen (Kinsey and Moerland, 2002). However, in the rainbow trout *Oncorhyncus mykiss*, the sarcolemmal of fast muscle fibres is relatively impermeable to lactate (Sharpe and Milligan, 2003), resulting in low rates of lactate efflux to the circulation during the recovery period (Milligan and Wood, 1986). Instead, lactate is retained within the muscle after exercise and used as a substrate for *in situ* glycogen resynthesis (Kieffler, 2000). Ultimately recovery of metabolism to the resting condition is dependent on oxidative phosphorylation. Although sites of SDHase localisation were more abundant in the periphery of fast muscle fibres in Arctic charr, some staining was observed in the central core, consistent with the presence of mitochondria (not shown). An ultrastructural study in the brook trout *Salvelinus fontinalis* also found mitochondria in the core of the largest diameter fast muscle fibres (Johnston and Moon, 1981). Thus, the maximum diameter of fast muscle fibres may well be limited by oxygen diffusion during recovery metabolism, reflecting the need to sustain these central mitochondria.

Myogenic progenitor cells and fibre recruitment

Myogenic regulatory factors (MRFs) belonging to the MyoD gene family play a pivotal role in specification of muscle lineage (MyoD and Myf-5) and in the initiation and stabilisation of the expression of muscle-specific genes (Myogenin, MRF4) in vertebrates (Rescan, 2001; Sabourin and Rudnicki, 2000). The MPCs in adult muscle express MRFs and differentiate into muscle nuclei, but are generally considered to develop from a pleuripotent stem cell population that under the right circumstances can also form adipocytes and chrondrocytes (Wada et al., 2002). In mouse, MPCs also express cell markers such as CD34 that are common to endothelial and haemopoietic stem cells as well as expressing m-cadherin, Pax 7 and Myf-5 (Tajbakhsh, 2003). Several lines of evidence point to a molecular heterogeneity of MPCs including; variation in the combination of markers expressed, differential labelling of MPCs *in vivo* and different proliferation rates of clonal cell lines (Zammit and Beauchamp, 2001; Tajbakhsh, 2003). Paired Box Protein 7 (Pax 7) is thought to be important for the maintenance of myogenic cells in mouse, and Pax 7 (–/–) knockouts lack muscle satellite cells (Seale et al., 2000). In the present study, cells immunopositive for Pax 7 constituted 3.2% of the total nuclei, which is similar to the proportion of myogenic cells in the fast muscle of other teleosts estimated using ultrastructural criteria (Koumans et al., 1991). Forkhead box protein (FoxK1) is a winged-helix transcription factor, which shows persistently high expression in mouse MPCs (Garry et al., 1997). In the mouse, FoxK1 occurs as two alternatively splice isoforms (α and β; Bassel-Duby et al., 1994; Yang et al., 1997). FoxK1-α is expressed in committed myoblasts and differentiated myoblasts whereas the expression of FoxK1-β is restricted to the early stages of differentiation (Yang et al., 1997). In Arctic charr, the majority of MPCs were committed to terminal differentiation and expressed FoxK1-α and MyoD. The density of cells staining for these markers was relatively constant over the body size range examined (Figs 12, 13). None of these markers is therefore specific to the founder myoblasts that are required to initiate new fibre production, and such cells may be relatively rare. The number of nuclei increased with fibre diameter, reaching 5000 cm^{-1} in 180 μm diameter fast muscle fibres (Fig. 11C). It is apparent that the vast majority of MPCs in fish are absorbed into fibres as they expand in diameter or are involved in nuclear turnover. The transcription factor NFATc2, which is only expressed in nascent myotubes in the mouse, was shown to activate myoblast–myotube fusion by activating the cytokine IL-4. Myoblasts that expressed the IL-4a receptor responded to IL-4 signals from the fibre, leading to further fusion and increase in myotube size (Horsley et al., 2003). There are no known phenotypic markers of the founder myoblasts that initiate myotube formation in fish, although the

orthologue of the IL-4a receptor is a promising candidate. It is not known whether the founder myoblasts for myotube formation originate early in development or are derived from the general pool of proliferating MPCs in response to local signalling from the muscle fibres (see Johnston et al., 2003b). The recent completion of several fish genome sequences should greatly facilitate the identification of gene networks regulating myotube formation, including the discovery of novel genes.

The monoclonal antibody S58 developed by Frank Stockdale was obtained from the Developmental Studies Hybridoma Bank developed under the auspices of the NICHD and maintained by The University of Iowa, Department of Biological Sciences, Iowa City, IA 52242, USA. We are grateful to all the staff at Holar College and particularly to Helgi Thorarensen and Rán Sturlaugsdóttir who helped with the rearing of fish and the rearing experiments. This work was made possible by a grant (NER/A/S/2000/00558) from the Natural Environment Research Council of the UK.

References

Abercromby, M. (1946). Estimation of nuclear population from microtome sections. *Anat Rec*. **94**, 239-247.

Ayala, M. D., López-Albors, O., Gil, F., Latorre, R., Vázquez, J. M., García-Alcázar, A., Abellán, E., Ramírez, G. and Moreno, F. (2000). Temperature effect on muscle growth of the axial musculature of the sea bass (*Dicentrarchus labrax* L.). *Anat. Histol. Embryol*. **29**, 235-241.

Bargelloni, L., Ritchie, P. A., Patarnello, T., Battaglia, B., Lambert, D. M. and Meyer, A. (1994). Molecular evolution at subzero temperatures: mitochondrial and nuclear phylogenies of fishes from AntArctica (suborder Notothenioidei), and the evolution of antifreeze glycopeptides. *Mol. Biol. Evol*. **11**, 854-863.

Bargelloni, L., Marcato, S., Zane, L. and Patarnello, T. (2000). Mitochondrial phylogeny of notothenioids: a molecular approach to AntArctic fish evolution and biogeography. *Syst. Biol*. **49**, 114-129.

Barresi, M. J., D'Angelo, J. A., Hernandez, L. P. and Devoto, S. H. (2001). Distinct mechanisms regulate slow muscle development. *Curr. Biol*. **11**, 1432-1438.

Bassel-Duby, R., Hernandez, M. D., Yang, Q., Rochelle, J. M., Seldin, M. F. and Williams, R. S. (1994). Myocyte nuclear factor, a novel winged-helix transcription factor under both developemtal and neural regulation in striated myocytes. *Mol. Cell. Biol*. **14**, 4596-4605.

Blagden, C. S., Currie, P. D., Ingham, P. W. and Hughes, S. (1997). Notochord induction of zebrafish slow muscle mediated by Sonic hedgehog. *Genes Dev*. **11**, 2163-2175.

Bowman, A. W. and Azzalini, A. (1997). *Applied Smoothing Techniques For Data Analysis. The Kernel Approach With S-Plus Illustrations.* Oxford Science Publications. pp193. Oxford: Oxford University Press.

Brunner, P. C., Douglas, M. R., Osinov, A., Wilson, C. C. and Bernatchez, L. (2001). HolArctic phylogeography of Arctic charr (*Salvelinus alpinus* L.) inferred from mitochondrial DNA sequences. *Evolution*. **55**, 573-586.

Calvo, J. (1989). Sexual differences in the increase in white muscle fibres in Argentinian hake (*Merluccius hubbsi*) from the San Matias Gulf (Argentina). *J. Fish Biol*. **35**, 207-214.

Clarke, A. and Johnston, N. M. (1999). Scaling of metabolic rate with body mass and temperature in teleost fish. *J. Animal Ecol*. **68**, 893-905.

Clausen, T. (2003). Na^+K^+ pump regulation and skeletal muscle contractility. *Physiol. Rev*. **83**, 1269-1324.

Crow, M. T. and Stockdale, F. E. (1986). Myosin expression and specialization amongst the earliest muscle fibres of the developing avian limb. *Dev. Biol*. **113**, 238-254.

Devoto, S. H., Melancon, E., Eisen, J. S. and Westerfield, M. (1996). Identification of separate slow and fast muscle precursors *in vivo*, prior to somite formation. *Development* **122**, 3371-3380.

Egginton, S., Skilbeck, C., Hoofd, L., Calvo, J. and Johnston, I. A. (2002). Peripheral oxygen transport in skeletal muscle of AntArctic and sub-AntArctic notothenioid fish. *J. Exp. Biol*. **205**, 769-779.

Eggleton, C. D., Vadapalli, A., Roy, T. K. and Popel, A. S. (2000). Calculations of intracapillary oxygen tension distributions in muscle. *Math. Biosci.* **167**, 123-143.

Eiríksson, G. M., Skúlason, S. and Snorrason, S. (1999). Heterochrony in skeletal development and body size in progeny of two morphs of Arctic charr from Thingvallavatn, Iceland. *J. Fish Biol*. **55**, 175-185.

Ennion, S., Wilkes, D., Gauvry, L., Alami-Durante, H. and Goldspink, G. (1999). Identification and expression analysis of two developmentally regulated myosin heavy chain gene transcripts in carp (*Cyprinus carpio*). *J. Exp. Biol*. **202**, 1081-1090.

Feldman, J. L. and Stockdale, F. E. (1991). Skeletal muscle satellite cell diversity:satellite cells form fibers of different types in cell culture. *Dev. Biol*. **143**, 320-334.

Garry, D. J., Yang, Q., Bassel-Duby, R. and Williams, R. S. (1997). Persistent expression of MNF identifies myogenic stem cells in postnatal muscles. *Dev. Biol*. **188**, 280-294.

Gíslason, D., Ferguson, M. M., Skúlason, S. and Snorrason, S. S. (1999). Rapid and coupled phenotypic and genetic divergence in Icelandic Arctic charr (*Salvelinus alpinus*). *Can. J. Fish. Aquat. Sci*. **56**, 2229-2234.

Hawke, T. J. and Garry, D. J. (2001). Myogenic satellite cells: physiology to molecular biology. *J. Appl. Physiol*. **91**, 534-551.

Hendry, A. P., Wenburg, J. K., Bentzen, P., Volk, E. C. and Quinn, T. P. (2000). Rapid evolution of reproductive isolation in the wild: Evidence from introduced salmon. *Science* **290**, 516-518.

Hill, A. V. (1965). The diffusion of oxygen through tissues. In *Trials and Trails in Physiology*, pp 208-241. London: Edward Arnold.

Hochachka, P. W. (1985). Fuels and pathways as designed systems for support of muscle work. *J. Exp. Biol*. **115**, 149-164.

Horsley, V., Jansen, K. M., Mills, S. T. and Pavlath, G. K. (2003). IL-4 acts as a myoblast recruitment factor during mammalian muscle growth. *Cell* **113**, 483-494.

Jobling, M. (1994). *Fish Bioenergetics*. London: Chapman and Hall.

Johnson, L. (1980). The Arctic charr, *Salvelinus alpinus*. In *Charrs, Salmonid Fishes of the Genus Salvelinus* (ed. E.K. Balon), pp.15-98. The Hague: Junk.

Johnston, I. A. (2003). Muscle metabolism and growth in AntArctic fishes suborder Notothenioidei): evolution in a cold environment. *Comp. Biochem. Physiol.* **136B**, 701-713.

Johnston, I. A. and Hall, T. E. (2004). Mechanisms of muscle development and responses to temperature change in fish larvae. In *The Development of Form and Function in Fishes and the Question of Larval Adaptation. American Fisheries Society Symp*. 40 (ed. J. J. Govoni), pp. 113-144. Bethesda, Maryland: American Fisheries Society.

Johnston, I. A. and McLay, H. A. (1997). Temperature and family effects on muscle cellularity at hatch and first feeding in Atlantic salmon (*Salmo salar* L.). *Can J. Zool*. **75**, 64-74.

Johnston, I. A. and Moon, T. W. (1981). Fine structure and metabolism of multiply innervated fast muscle fibres in teleost fish. *Cell Tissue Res*. **219**, 93-109.

Johnston, I. A., Patterson, S., Ward, P. and Goldspink, G. (1974). The histochemical demonstration of myofibrillar adenosine triphosphatase activity in fish muscle. *Can. J. Zool*. **52**, 871-877.

Johnston, I. A., Patterson, S., Ward, P. and Goldspink, G. (1975). Studies on the swimming musculature of the rainbow trout. I. Fibre types. *J. Fish Biol*. **7**, 451-458.

Johnston, I. A., Davison, W. and Goldspink, G. (1977). Energy metabolism of carp swimming muscles. *J. Comp. Physiol. B* **114**, 203-216.

Johnston, I. A., Vieira, V. L. A. and Abercromby, M. (1995). Temperature and myogenesis in embryos of the Atlantic herring, *Clupea harengus*. *J. Exp. Biol*. **198**, 1389-1403.

Johnston, I. A., Cole, N. J., Vieira, V. L. A. and Davidson, I. (1997). Temperature and developmental plasticity of muscle phenotype in herring larvae. *J. Exp. Biol.* **200**, 849-868.

Johnston, I. A., Cole, N. J., Abercromby, M. and Vieira, V. L. A. (1998). Embryonic temperature modulates muscle growth characteristics in larval and juvenile herring. *J. Exp. Biol.* **201**, 623-646.

Johnston, I. A., Strugnell, G., McCracken, M. L. and Jonstone, R. (1999). Muscle growth and development in normal-sex-ratio and all-female diploid and triploid Atlantic salmon. *J. Exp. Biol*. **202**, 1991-2016.

Johnston, I. A., McLay, H. A., Abercromby, M. and Robins, D. (2000a). Phenotypic plasticity of early myogenesis and satellite cell numbers in Atlantic salmon spawning in upland and lowland tributaries of a river system. *J. Exp. Biol*. **20**3, 2539-2552.

Johnston, I. A., McLay, H. A., Abercromby, M. and Robins, D. (2000b). Early thermal experience has different effects on growth and muscle fibre recruitment in spring- and autumn-running Atlantic salmon populations. *J. Exp. Biol*. **203**, 2553-2564.

Johnston, I. A., Manthri, S., Robertson, B., Campbell, P., Mitchell, D. and Alderson, R. (2000c). Family and population differences in muscle fibre recruitment in farmed Atlantic salmon (*Salmo salar*). *Basic Appl. Myol*. **10**, 291-296.

Johnston, I. A., Fernandez, D., Calvo, J., Vieira, V. L. A., North, A. W., Abercromby, M. and Garland, T., Jr (2003a). Reduction in muscle fibre number during the adaptive radiation of notothenioid fishes: a phylogenetic perspective. *J. Exp. Biol*. **206**, 2595-2609.

Johnston, I. A., Hall, T. E. and Fernández, D. A. (2003b). Genes regulating the growth of myotomal muscle in teleost fish. In *Aquatic Genomics – Steps Towards a Great Future* (ed. N. Shimizu, T. Aoki, I. Hirano and F. Takashima), pp. 53-166. Tokyo: Springer-Verlag.

Johnston, I. A., Manthri, S., Alderson, R., Smart, A., Campbell, P., Nickell, D., Robertson, B., Paxton, C. G. M. and Burt, M. L. (2003c). Freshwater environment affects growth rate and muscle fibre recruitment in seawater stages of Atlantic salmon (*Salmo salar* L.). *J. Exp. Biol*. **206**, 1337-1351.

Johnston, I. A., Manthri, S., Smart, A., Campbell, P., Nickell, D. and Alderson, R. (2003d). Plasticity of muscle fibre number in seawater stages of Atlantic salmon in response to photoperiod manipulation. *J. Exp. Biol*. **206**, 3425-3435.

Jonsson, B. (1976). Comparison of scales and otoliths for age determination in brown trout *Salmo trutta* L. *Norw. J. Zool*. **24**, 295-301.

Keiffer, J. (2000). Limits to exhaustive exercise in fish. *Comp. Biochem. Physiol*. **126A**, 161-179.

Kinsey, S. T. and Moerland, T. S. (2002). Metabolic diffusion in giant muscle fibres of the spiny lobster *Panulirus argus*. *J. Exp. Biol*. **205**, 3377-3386.

Koumans, J. T. M., Akster, H. A., Brooms, G. H. R., Lemmens, C. J. J. and Osse, J. W. M. (1991). Numbers of myosatellite cells in white axial muscles of growing fish, *Cyprinus carpio* L. (Teleostei). *Am. J. Anat*. **192**, 418-424.

Levin, J. M., El Andalousi, R. A. B., Dainat, J., Reyne, Y. and Bacou, F. (2001). SFRP2 expression in rabbit myogenic progenitor cells and in adult skeletal muscles. *J. Musc. Res. Cell Motil*. **22**, 361-369.

Milligan, C. L. and Wood, C. M. (1986). Tissue intracellular acid-base status and the fate of lactate after exhaustive exercise in rainbow trout. *J. Exp. Biol*. **123**, 123-144.

Mootoosamy, R. C. and Dietrich, S. (2002). Distinct regulatory cascades for head and trunk myogenesis. *Development* **129**, 573-583.

Myers, R. A., Hutchings, J. A. and Gibson, R. J. (1986). Variations in male parr maturation within and among populations of Atlantic salmon, *Salmo salar*. *Can. Fish. Aquat. Sci*. **43**, 1242-1248.

Nachlas, M. M., Tsou, K. C., de Souza, E., Cheng, C. S. and Seligman, A. M. (1957). Cytochemical demonstration of succinic dehydrogenase by the use of a new p-nitrophenyl substituted dietrazole. *J. Histochem. Cytochem*. **5**, 420-436.

Nordeng, H. (1983). Solution to the 'charr problem' based on Arctic charr (*Salvelinus alpinus*) in Norway. *Can. J. Fish. Aquat. Sci*. **40**, 1372-1387.

Nyman, L., Hammar, J. and Gydemo, R. (1981). The systematics and biology of landlocked populations of Arctic charr from Northern Europe. Rep. *Inst. Freshwat. Res. Drottingholm* **59**, 128-141.

Pearse, A. G. E. (1960). *Histochemistry*, 2nd Edition. Town: Churchill Livingstone.

Rescan, P. Y. (2001). Regulation and function of myogenic regulatory factors in lower vertebrates. *Comp. Biochem. Physiol. B* **130**, 1-12.

Richards, J. G., Heigenhauser, G. J. F. and Wood, C. M. (2002). Glycogen phosphorylase and pyruvate dehydrogenase transformation in white muscle of trout during high intensity exercise. *Am. J. Physiol*. **282**, R828-836.

Rowlerson, A. and Veggetti, A. (2001). Cellular mechanisms of post-embryonic muscle growth in aquaculture species. In *Muscle Development and Growth*. *Fish Physiology*, vol. 18 (ed. I. A. Johnston), pp. 103-140. San Diego: Academic Press.

Rowlerson, A., Mascarello, F., Radaelli, G. and Veggetti, A. (1995). Differentiation and growth of muscle in the fish *Sparus aurata* (L.): II Hyperplastic and hypertrophic growth of lateral muscle from hatching to adult. *J. Muscle Res. Cell Motil*. **16**, 223-236.

Rudnicki, M. A. and Jaenisch, R. (1995). The MyoD family of transcription factors and skeletal myogenesis. *BioEssays* **17**, 203-209.

Sabourin, L. A. and Rudnicki, M. A. (2000). The molecular regulation of myogenesis. *Clin. Genet.* **57**, 16-25.

Saemundsson, K. (1992). Geology of the Thingvallavatn area. *Oikos* **64**, 40-68.

Salathe, E. P. and Gorman, A. D. (1997). Modelling oxygen concentration in skeletal muscle. *Math. Comput. Modelling* **26**, 91-102.

Sandlund, O. T., Gunnarsson, K., Jónasson, P. M., Jonsson, B., Lindem, T., Magnússon, K. P., Malmquist, H. J., Sigurjónsdóttir, H., Skúlason, S. and Snorrason, S. (1992). The Arctic charr *Salvelinus alpinus* in Thingvallavatn. *Oikos* **64**, 305-351.

Schaffer, W. M. and Elson, P. F. (1975). The adaptive significance of variations in life history among local populations of Atlantic salmon in North America. *Ecol.* **56**, 291-303.

Seale, P. L. A., Sabourin, A., Girgis-Gabardo, A., Mansouri, A., Gruss, P. and Rudnicki, M. A. (2000). Pax 7 is required for the specification of myogenic satellite cells. *Cell* **102**, 777-786.

Sharpe, R. L. and Milligan, C. L. (2003). Lactate efflux from sarcolemmal vesicles isolated from rainbow trout *Oncorhynchus mykiss* white muscle is via simple diffusion. *J. Exp. Biol*. **206**, 543-549.

Sidell, B. D. (1998). Intracellular oxygen diffusion: The roles of myoglobin and lipid at cold body temperature. *J. Exp. Biol*. **201**, 1119-1128.

Skúlason, S. and Smith, T. B. (1995). Resource polymorphism in vertebrates. *Trends Ecol. Evol.* **10**, 366-370.

Skúlason, S., Snorrason, S. S., Noakes, D. L. G., Ferguson, M. M. and Malmquist, H. J. (1989a). Segregation in spawning and early life history among polymorphic Arctic charr *Salvelinus alpinus*, in Thingvallavatn, Iceland. *J. Fish Biol*. **35**, 225-232.

Skúlason, S., Noakes, D. L. G. and Snorrason, S. S. (1989b). Ontogeny of trophic morphology in four sympatric morphs of Arctic charr, Salvelinus alpinus, in Thingvallavatn, Iceland. *Biol. J. Linn. Soc*. **38**, 281-301.

Skúlason, S., Snorrason, S. S., Ota, D. and Noakes, D. L. G. (1993). Genetically based differences in foraging behaviour among sympatric morphs of Arctic charr (Pisces; Salmonidae). *Anim. Behav*. **45**, 1179-1192.

Skúlason, S., Snorrason, S. S., Noakes, D. L. G. and Ferguson, M. M. (1996). Genetic basis of life history variations among sympatric morphs of Arctic charr *Salvelinus alpinus*. *Can. J. Fish. Aquat. Sci.* **53**, 1807-1813.

Skúlason, S., Snorrason, S. S. and Jónsson, B. (1999). Sympatric morphs, populations and speciation in freshwater fish with emphasis on Arctic charr. pp. 70-92. In *Evolution of Biological Diversity* (ed. A. E. Magurran and R. M. May) Oxford: Oxford University Press.

Smialowska, E. and Kilarski, W. (1981). Histological analysis of fibers in myotomes of AntArctic fish (Admiralty Bay, King George Island, South Shetland Islands). I. Comparative analysis of muscle fiber size. *Pol. Polar Res*. **2**, 109-129.

Snorrason, S. S. and Skúlason, S. (2004). Adaptive speciation in northern freshwater fishes – patterns and processes. In *Adaptive Speciation* (ed. U. Dieckmann, H. Metz, M. Doebeli and D. Tautz). Cambridge, UK: Cambridge University Press (in press).

Snorrason, S. S., Skúlason, S., Jonsson, B., Malmquist, H. J. and Jónasson, P. M. (1994). Trophic specialisation in Arctic charr *Salvelinus alpinus* (Pices: Salmonidae): morphological divergence and ontogenetic niche shifts. *Biol. J. Linn. Soc*. **52**, 1-18.

Stankovic, A., Spalik, K., Kamler, E., Borsuk, P. and Weglenski, P. (2001). Recent origin of sub-AntArctic notothenioids. *Polar Biol.* **25**, 203-205.

Stickland, N. C. (1983). Growth and development of muscle fibres in the rainbow trout (*Salmo gairdneri*). *J. Anat.* **137**, 323-333.

Stickland, N. C., White, R. N., Mescall, P. E., Crook, A. R. and Thorpe, J. E. (1988). The effect of temperature on myogenesis in embryonic development of the Atlantic salmon (*Salmo salar* L.). *Anat. Embryol.* **178**, 253-257.

Tajbakhsh, S. (2003). Stem cells to tissue: molecular, cellular and anatomical heterogeneity in skeletal muscle. *Curr. Opin. Gen. Dev*. **13**, 413-422.

Van Raamsdonk, W., Mos, W., Smit-Onel, M. J., van der Laarse, W. J. and Fehres, R. (1983). The development of the spinal motor column in relation to the myotomal muscle fibers in the Zebrafish (*Brachydanio rerio*). I. Posthatching Development. *Anat. Embryol*. **167**, 125-139.

Wada, M. R., Inagawa-Ogashiwa, M., Shimuzu, S., Yaumoto, S. and Hashimoto, N. (2002). Generation of different fates from multipotent muscle stem cells. *Development* **129**, 2987-2995.

Weatherley, A. H., Gill, H. S. and Rogers, S. (1980). The relationship between mosaic muscle fibres and size in rainbow trout (*Salmo gairdneri*). *J. Fish Biol*. **17**, 603-610.

Weatherley, A. H., Gill, H. S. and Lobo, A. F. (1988). Recruitment and maximum diameter of axial muscle fibres in teleosts and their relationship to somatic growth and ultimate size. *J. Fish Biol*. **33**, 851-859.

Wilson, A. J., Gíslason, D., Skúlason, S., Snorrason, S., Adams, C. E., Alexander, G., Danzmann, R. G. and Ferguson, M. M. (2004). Population genetic structure of Arctic charr, *Salvelinus alpinus* from northwest Europe on large and small spatial scales. *Mol. Ecol.* **13**, 1129-1142.

Yang, Q., Bassel-Duby, R. and Williams, R. S. (1997). Transient expression of a winged-helix protein, MNF-B during myogenesis. *Mol. Cell. Biol.* **17**, 5236-5243.

Zammit, P. and Beauchamp, J. (2001). The skeletal muscle satellite cell: stem cell or son of stem cell? *Differentiation* **68**, 193-204.